View metadata, citation and similar papers at core.ac.uk
brought to you by CORE
provided by Ludovika Digital Knowledge Repository and Archive (LUDITA)

A&A 525, A109 (2011)
DOI: 10.1051/0004-6361/201015261
© ESO 2010

Astronomy & Astrophysics

Searching for differences in *Swift*'s intermediate GRBs

A. de Ugarte Postigo[1,2], I. Horváth[3], P. Veres[3,4], Z. Bagoly[4], D. A. Kann[5], C. C. Thöne[1], L. G. Balazs[6], P. D'Avanzo[1], M. A. Aloy[7], S. Foley[8,9], S. Campana[1], J. Mao[1,10,11], P. Jakobsson[12], S. Covino[1], J. P. U. Fynbo[13], J. Gorosabel[14], A. J. Castro-Tirado[14], L. Amati[15], and M. Nardini[9]

[1] INAF – Osservatorio Astronomico di Brera, via E. Bianchi 46, 23807 Merate, LC, Italy
e-mail: antonio.deugarte@brera.inaf.it
[2] European Southern Observatory, Casilla 19001, Santiago 19, Chile
[3] Dept. of Physics, Bolyai Military University, POB 15, 1581 Budapest, Hungary
[4] Dept. of Physics of Complex Systems, Eötvös University, Pázmány P. s. 1/A, 1117 Budapest, Hungary
[5] Thüringer Landessternwarte Tautenburg, Sternwarte 5, 07778 Tautenburg, Germany
[6] Konkoly Observatory, 1525 Budapest, POB 67, Hungary
[7] Departamento de Astronomía y Astrofísica, Universidad de Valencia, 46100 Burjassot, Spain
[8] UCD School of Physics, University College Dublin, Dublin 4, Ireland
[9] Max-Planck-Institut für extraterrestrische Physik, 85748 Garching, Germany
[10] Yunnan Observatory, Chinese Academy of Sciences, Kunming, Yunnan 650011, PR China
[11] Key Laboratory for the Structure and Evolution of Celestial Objects, Chinese Academy of Sciences, Yunnan 650011, PR China
[12] Centre for Astrophysics and Cosmology, Science Institute, University of Iceland, Dunhagi 5, 107 Reykjavik, Iceland
[13] Dark Cosmology Centre, Niels Bohr Institute, University of Copenhagen, Juliane Maries Vej 30, 2100 Copenhagen Ø, Denmark
[14] Instituto de Astrofísica de Andalucía (IAA-CSIC), 18008 Granada, Spain
[15] INAF – IASF Bologna, via P. Gobetti 101, 40129 Bologna, Italy

Received 22 June 2010 / Accepted 6 July 2010

ABSTRACT

Context. Gamma-ray bursts are usually classified in terms their high-energy emission into either short-duration or long-duration bursts, which presumably reflect two different types of progenitors. However, it has been shown on statistical grounds that a third, intermediate population is needed in this classification scheme, although an extensive study of the properties of this class has so far not been performed. The large amount of follow-up studies generated during the *Swift* era allows us to have a sufficient sample to attempt a study of this third population through the properties of their prompt emission and their afterglows.
Aims. To understand the differences of the intermediate population, we study a sample of GRBs observed by *Swift* during its first four years of operation. The sample contains only bursts with measured redshifts since these data help us to derive intrinsic properties.
Methods. We search for differences in the properties of the three groups of bursts, which we quantify using a Kolmogorov-Smirnov test whenever possible.
Results. Intermediate bursts are found to be less energetic and have dimmer afterglows than long GRBs, especially when considering the X-ray light curves, which are on average one order of magnitude fainter than long bursts. There is a less significant trend in the redshift distribution that places intermediate bursts closer than long bursts. Except for this, intermediate bursts show similar properties to long bursts. In particular, they follow the $E_{\rm peak}$ versus $E_{\rm iso}$ correlation and have, on average, positive spectral lags with a distribution similar to that of long bursts. As for long GRBs, they normally have an associated supernova, although some intermediate bursts have been found to contain no supernova component.
Conclusions. This study shows that intermediate bursts differ from short bursts, but exhibit no significant differences from long bursts apart from their lower brightness. We suggest that the physical difference between intermediate and long bursts could be explained by being produced by similar progenitors, of the former being the ejecta thin shells and the latter thick shells.

Key words. gamma-rays burst: general

1. Introduction

The classification of gamma-ray bursts (GRBs) has been a great challenge since their discovery in the late 1960s. Mazets et al. (1981) and Norris et al. (1984) suggested that they could be distinguished by the distributions of their durations. This became more obvious when Kouveliotou et al. (1993) found a clear bimodality in the duration histogram of GRBs using the first BATSE catalogue. Since then, it has been widely accepted that GRBs can be separated into *long* (T_{90}[1] longer than ~2 s) and *short* (T_{90} shorter than ~2 s) bursts. In addition, they showed that short bursts have harder spectra than long bursts. However, from the study of the BATSE GRB sample, Horváth (1998, 2002) and Mukherjee et al. (1998) independently suggested that the former classification was incomplete, estimating a probability of 10^{-4} of having only 2 classes. They concluded that the original long class should be separated further into a new intermediate class and a long class. This classification has also been proposed for the datasets of other satellites (Horváth 2009; Řípa et al. 2009; Horváth et al. 2010).

GRBs are usually explained within the context of the fireball model (Rees & Meszaros 1992; Daigne & Mochkovitch 1998; Sari et al. 1999), a progenitor-independent model that, in spite

[1] T_{90} is defined as the time during which the cumulative counts increase from 5% to 95% above background, adding up to 90% of the total GRB counts.

of some difficulties (Lyutikov 2009), is generally used as reference in the field to explain the burst itself and its afterglow. There are a variety of objects capable of generating the fireball: collapsars (Woosley 1993; Paczyński 1998), neutron star – neutron star mergers (Paczynski 1990), neutron star – black hole mergers (Narayan et al. 1992), or white dwarf – black hole mergers (Levan et al. 2006; Chattopadhyay et al. 2007; King et al. 2007). The most widely accepted idea is that long GRBs are generated by collapsars (characterised by the presence of a core-collapse supernova, Galama et al. 1998; Castro-Tirado & Gorosabel 1999; Hjorth et al. 2003; Stanek et al. 2003; Malesani et al. 2004; Pian et al. 2006), while short bursts are the result of compact binary mergers (with no supernova component, Gehrels et al. 2005; Hjorth et al. 2005a; Barthelmy et al. 2005; Berger et al. 2005c; Fong et al. 2010). Specific studies of the progenitors of the intermediate class based on afterglow observations have not yet been done.

Although the number of BATSE bursts was very large, there were too few afterglows detected to attempt a conclusive statistical analysis of the properties of each group. After the launch of *Swift* (Gehrels et al. 2004), follow-up studies became more efficient, thanks to the precise localisations by BAT and XRT and the fast distribution of their alerts. Four years after the detection of its first GRB, the *Swift* database had 394 bursts, of which 40% have measured redshifts. This rapidly growing sample has allowed statistical studies to be performed of the short and long population of bursts (Kann et al. 2010, 2008; Gehrels et al. 2008; Nysewander et al. 2009). In this paper, we use the sample of the first four years of *Swift* GRBs with known redshifts to search for the specific properties of the intermediate population, trying to evaluate whether any significant difference with respect to the other groups exists.

In Sect. 2, we provide details of the sample selected for this study. Section 3 compares the different properties of the three groups detailed in several subsections. Section 4 discusses the physical differences between intermediate and long bursts. Finally in Sect. 5 we present the discussion and conclusions of our work.

2. Sample selection and method

We use a sample that comprises all the bursts detected by *Swift* during the first four years since the detection of the first GRB by the satellite (i.e. from December 17, 2004 to December 17, 2008). For each of these bursts, we estimate the probability of belonging to a specific population by using the classification given by Horváth et al. (2010). Their method is based on a clustering analysis of the distribution of GRBs in the spectral hardness-ratio (HR) versus T_{90} diagram, where they find that the distribution is best-fit by three bidimensional Gaussians. From this result, they can derive, for each point of the diagram, a probability of belonging to each of the three groups. However, not all bursts have all the information needed for an accurate classification, which reduces the final sample to 325 bursts (the same sample as the one used by Horváth et al. 2010). In our study, we concentrate on bursts with measured redshifts or at least a redshift estimate. The characteristics of those bursts are summarised in Table 1.

The fuzzy-logic classification that we use, assigning a probability of belonging to each group according to the location in the HR vs. T_{90} duration diagram, implies some inherent contamination. In the sample of 325 *Swift* bursts (Horváth et al. 2010), 214 (66%) bursts are long, 86 (26%) are intermediate, and 25 (8%) are short. If we consider that a burst belongs to the group that has the highest probability, we expect to end up with 26 short-classified bursts (24 real-shorts and 2 misclassified-intermediates), 94 intermediate-classified bursts (73 real-intermediates, 1 misclassified-short and 20 misclassified-longs), and 205 long-classified bursts (194 real-longs and 11 misclassified-intermediates). The effect of the contamination can be reduced by increasing the threshold with which we classify the bursts. If we require a probability of 68% to assign a burst to a group and ignore the border events, we are left with 292 bursts, 25 short-classified bursts (24 real-shorts and 1 misclassified-intermediate), 77 intermediate-classified bursts (62 real-intermediates and 15 misclassified-longs), and 190 long-classified bursts (185 real-longs and 5 misclassified-intermediates). By going to a 90% probability threshold, we are left with 219 bursts, 22 short-classified bursts (all real-shorts), 49 intermediate-classified bursts (44 real-intermediates and 5 misclassified-longs), and 148 long-classified bursts (147 real-longs and 1 misclassified-intermediate). To eliminate the overlap between the different groups, while keeping a significant amount of events, we select as members of a group (unless specifically noted) only those that have a probability of more than 68% of belonging to it.

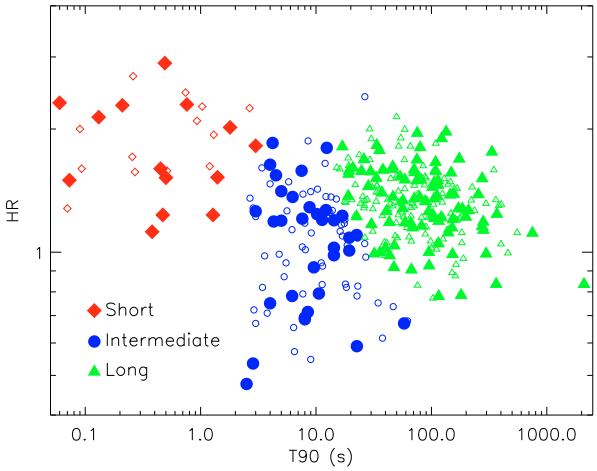

Fig. 1. HR vs. T_{90} diagram, as classified by Horváth et al. (2010). Short bursts are represented by red diamonds, long bursts with green triangles, and intermediate bursts with blue circles. Large filled symbols represent the GRBs for which there is a redshift, while small empty symbols are the remaining bursts of the *Swift* sample. A colour version of this figure can be found in the online version.

It has been shown that some short bursts are assigned a longer duration because of extended emission that is detectable only in the softest bands (Norris & Bonnell 2006; Norris et al. 2010). This can exacerbate misclassification of events. In this paper, we choose to classify those bursts using only the properties of the initial spike whenever possible.

The sample of bursts with known redshifts contains 137 bursts. Within this sample, there are 13 short, 28 intermediate, and 82 long bursts. The remaining (14) lie within the borders of the different groups, so that no group can be clearly assigned to them using the criteria described before. Figure 1 shows the distribution of *Swift* bursts in a plot of HR vs. T_{90}, highlighting those that have redshifts, on which we focus our study. The HR is defined as the ratio of the fluence recorded in the 50−100 keV to that in the 25−50 keV channels, while the duration is measured by the parameter T_{90}, the time span containing 90% of the flux.

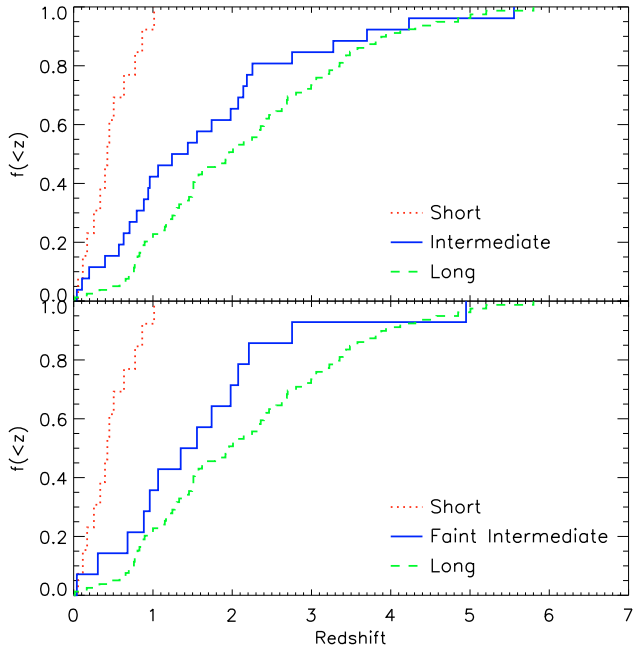

Fig. 2. Cumulative redshift distribution of the *Swift* sample of GRBs with redshift estimation. *Top*: using the full intermediate burst sample, short bursts show a clearly different distribution, while intermediate and long bursts are more difficult to discriminate between. *Bottom*: using only the faint intermediate bursts.

Throughout the paper, we select several parameters that we use to compare the properties of the different burst populations. To evaluate the significance of any differences in these parameters, we use a Kolmogorov-Smirnov (K-S) test whenever possible.

Throughout the paper we assume a cosmology with $\Omega_\Lambda = 0.7$, $\Omega_M = 0.3$, and $h = 0.73$.

3. Results

In the next section, we consider a number of observational characteristics of the GRBs in our sample and look for any differences between the three types. For clarity, we consistently plot short bursts with red dotted lines or diamond-shaped symbols, long bursts with green dashed lines or triangles, and intermediate bursts with continuous blue lines or circles, as shown in Figs. 1 and 2 (colours are displayed in the electronic version of the paper). A summary of the results of the different K-S tests can be found in Table 4. Table 5 provides median values and standard deviations of a number of the parameters studied.

3.1. Redshift distribution

Studying the BATSE sample of GRBs, Mészáros et al. (2000) found that intermediate bursts exhibited a non-randomness in their spatial distribution with a confidence of 96.4% (Vavrek et al. 2008, confirmed this result with a confidence of 98.5%). Furthermore, when selecting only the dimmer half of the intermediate burst sample this probability increased to 99.3%. This may be indicative of a different redshift distribution of this group of events. We now test this hypothesis.

Using the sample of *Swift* bursts with redshifts, we create cumulative distributions of bursts belonging to each of the groups, as shown in Fig. 2 (top). For short bursts, we measure an average (median) redshift of 0.50 (0.44), for intermediate bursts of 1.80 (1.55), and for long bursts we measure 2.21 (1.97). Both the cumulative graph and the average values show a clear difference between the short bursts and the long or intermediate bursts. The difference between intermediate and long bursts is, if existent, far more subtle. Using K-S statistics, we find that the probability of short and long bursts being drawn from the same underlying population is only 9.5×10^{-5}%, and 0.15% if we consider short and intermediate bursts. This confirms that the redshift distribution of short bursts clearly differs from that of intermediate or long bursts. On the other hand, the hypothesis of having the same distribution for intermediate and long bursts has a probability of 14% implying that, although there is a tendency for intermediate GRBs to be found at lower redshifts than long bursts, the statistical significance is still low.

As a further test, we compare the distribution of the dimmer intermediate bursts with that of the long bursts, because this pair of distributions were found by Mészáros et al. (2000) to exhibit the strongest difference. To do this, we select the fainter 50% of the bursts, defined as those bursts with a fluence in the 15−25 keV band lower or equal to the median value of all the intermediate bursts (the same result is obtained by using the 50−100 keV band). Using this subgroup, we obtain an average (median) redshift of 1.85 (1.56). The lower panel of Fig. 2 shows the cumulative distribution for only the dim bursts of the intermediate group. We see that the distribution does not differ significantly from that for the complete sample. The probability that long bursts and dim intermediate bursts have the same redshift distributions is 19%, implying an even less significant difference, probably because of the smaller sample size of the dim bursts.

3.2. X-ray afterglows

We next compare the afterglow luminosities of the different burst populations. To compare the intrinsic luminosities of the different bursts, we obtain the X-ray light curves of all the GRBs observed by *Swift*/XRT for which there is a redshift measurement and an estimate of the spectral slope and hydrogen column density (so that an unabsorbed flux can be derived). Using solely XRT data (Evans et al. 2007, 2009) has the advantage of ensuring the minimum amount of observational biases. The observations are not critically affected by either extinction, an underlying host galaxy, or a supernova component. Furthermore, a substantial percentage of the bursts have a detected afterglow. We use Eq. (2) of Ghisellini et al. (2009) to convert the flux measured by XRT to luminosities.

Figure 3 shows the light curves of the different GRB populations. In agreement with previous studies (Gehrels et al. 2008; Nysewander et al. 2009) and although the amount of short burst light curves is limited, the short population bursts are clearly fainter on average than the other two groups. Comparing intermediate and long bursts, we see that there is also a bimodality in the luminosity distribution with intermediate bursts being on average one order of magnitude fainter.

To evaluate the significance of this result, we apply a K-S test using the afterglow luminosity at two different epochs. The first epoch is taken at 10^2 s, when the light curve may be strongly affected by the early emission. We define the second epoch to occur at 10^4 s, when we can consider the light curve to be dominated by the afterglow. To obtain the luminosity at a given time, we apply a linear fit to all the measurements within one dex of the desired epoch. Figure 4 shows a histogram with the values for both epochs.

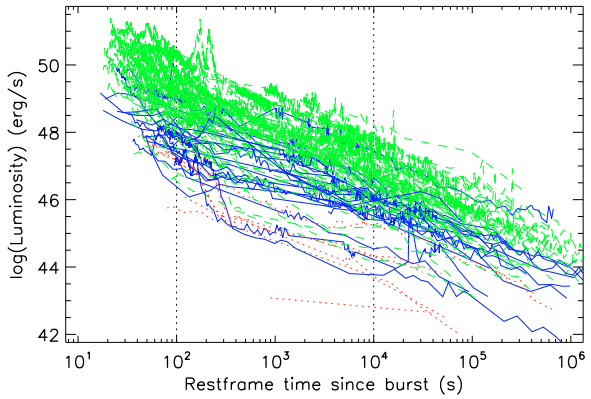

Fig. 3. X-ray afterglow luminosities of the different burst populations. The vertical lines mark 10^2 and 10^4 s, where we obtain the histograms. Each group is identified with the same line styles and colours as in Fig. 2.

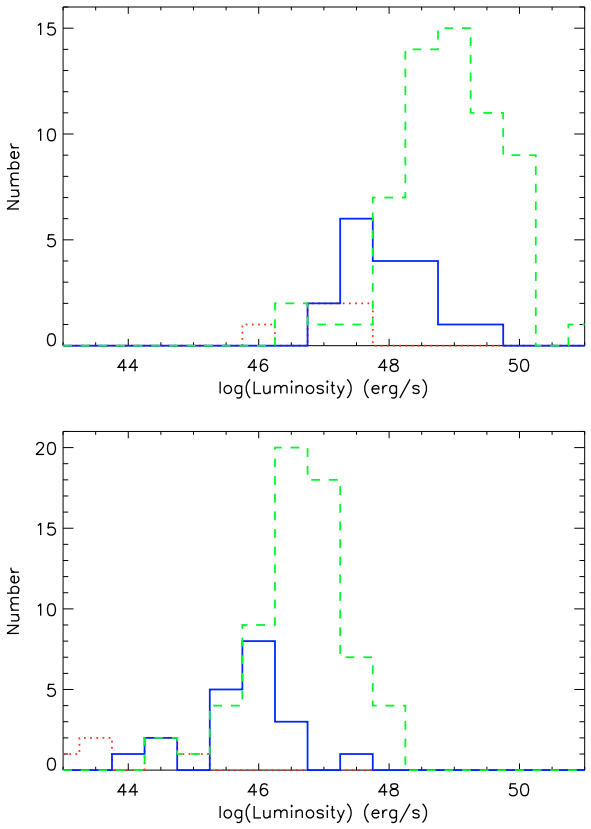

Fig. 4. Histograms showing the distribution of X-ray luminosities 10^2 s after the GRB trigger (*top panel*) and 10^4 s after the GRB trigger (*bottom panel*). Each group is identified with the same line styles and colours as in Fig. 2.

For the histogram at 10^2 s, we measure an average (median) logarithm of the luminosity of short bursts of 47.0 (47.2) with a standard deviation of 0.6. For intermediate bursts, we measure 47.9 (47.9) with a standard deviation of 0.6. For long bursts, the value is 49.1 (49.1) with a standard deviation of 1.6. The K-S test rejects the hypothesis of having the same luminosity distribution for intermediate and long bursts with a probability of 0.005% that their distributions are drawn from the same population, for short and intermediate bursts this probability is 1.6%, and for short and long bursts it is 0.02%. At 10^4 s, we find that the average (median) logarithm of the luminosity for short bursts

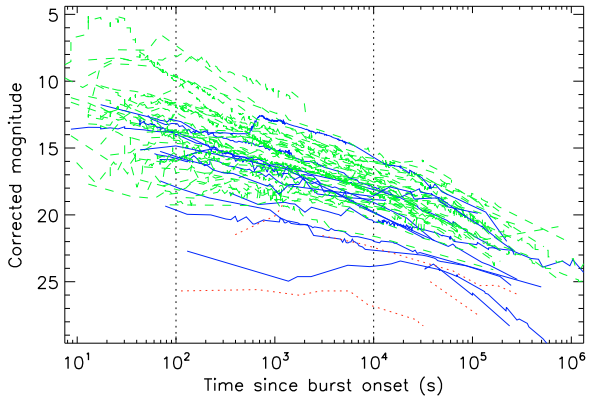

Fig. 5. Optical afterglow light curves of the different burst populations as observed if placed at redshift $z = 1$. The vertical lines mark the two epochs at 10^2 and 10^4 s, which we use to obtain the histograms in Fig. 6. Each group is identified with the same line styles and colours as in Fig. 2.

is 44.0 (44.4) with a standard deviation of 0.8. For intermediate bursts, it is 45.8 (46.0) with a standard deviation of 0.7, while for long bursts we meassure 46.6 (46.7) with a standard deviation of 0.7. When applying the K-S test, we find that the hypothesis of having the same luminosity distribution at 10^4 s for intermediate and long bursts has a probability of 0.007%, strongly rejecting this possibility. For intermediate and short bursts, the probability is 0.08% and for short and long bursts 0.002%. We note that for short bursts we have limited data, thus the numbers that we derive are not very significant.

In both cases, we see that the X-ray afterglow luminosity distributions for intermediate and long bursts can be distinguished with strong confidence. We also note that the difference in luminosity is greater for the first epoch where the early component of long GRB light curves seems to be stronger than the intermediate burst one.

3.3. Optical afterglows

We repeat the analysis of the X-ray afterglows for the optical afterglows, using the magnitudes derived by Kann et al. (2010, 2008, see Fig. 5). These authors corrected the afterglow magnitudes for Galactic and host galaxy extinction and placed them at a common redshift of $z = 1$ to allow a direct comparison of their intrinsic properties. The number of short afterglows in our sample is too small to allow us to derive significant conclusions, so in this section we concentrate only on intermediate and long bursts (see Fig. 6). At 10^2 s, the average (median) magnitude of intermediate bursts is 15.5 (15.6) with a dispersion of 2.0 mag. For long bursts it is 13.7 (13.8) with a dispersion of 2.9 mag. The K-S test gives the same population hypothesis a 11% probability. At 10^4 s, the average (median) magnitude of intermediate bursts is 19.7 (19.8) with a dispersion of 2.3 mag. For long bursts, it is 18.0 (18.1) with a dispersion of 1.4 mag. The K-S test assigns to the same population hypothesis a 3.3% probability. This indicates that for the optical afterglows, the difference we detected for the X-ray afterglows, while not as significant, is still present.

We note that there are no intermediate bursts with extremely bright optical peak emission, whereas there are a few cases for long bursts (Akerlof et al. 1999; Boër et al. 2006; Jelínek et al. 2006; Kann et al. 2007; Bloom et al. 2009; Racusin et al. 2008). This may be indicative of differences in the characteristics or close environment of the progenitors producing the GRB but it

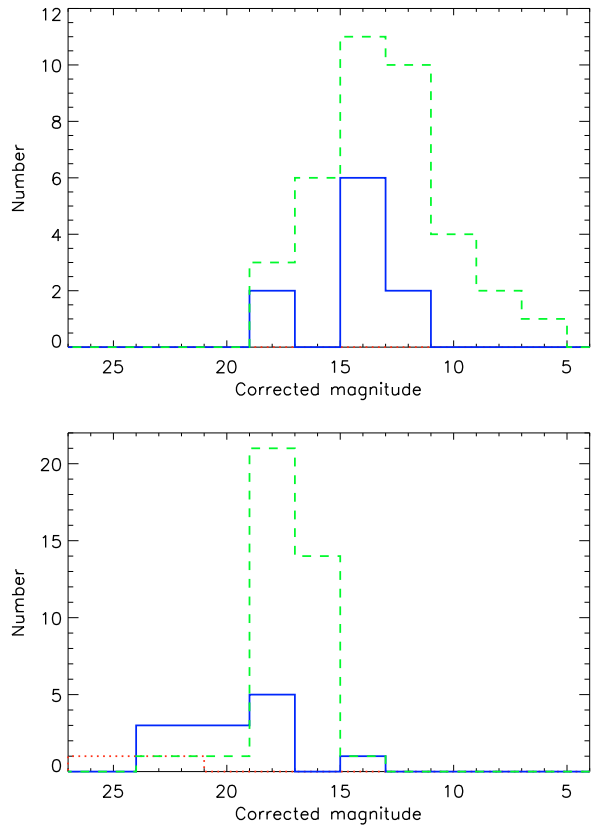

Fig. 6. Histograms showing the distribution of optical luminosities 10^2 s after the GRB trigger (*top panel*) and 10^4 s after the GRB trigger (*bottom panel*). Each group is identified with the same line styles and colours as in Fig. 2.

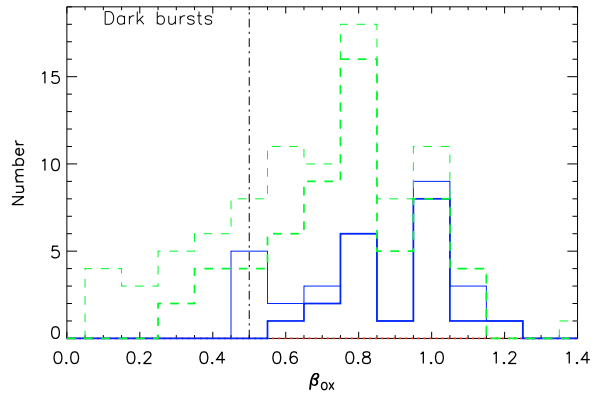

Fig. 7. Histogram showing the distribution of the spectral slope between optical and X-rays. In this case, we also plot detection limits. The horizontal line marks the limit between optically dark bursts ($\beta_{OX} < 0.5$) and bright bursts. Each group is identified with the same line styles and colours as in Fig. 2, where thick lines indicate detections and thin ones are detection limits.

might also simply be an effect of low number statistics in the intermediate burst sample.

3.4. Distribution of dark bursts

The distribution of the spectral slope between the optical and X-rays (β_{OX}) identifies optically dark bursts as those with $\beta_{OX} < 0.5$ (Jakobsson et al. 2004). In Fig. 7, we show the distribution according to the different groups obtained using the method

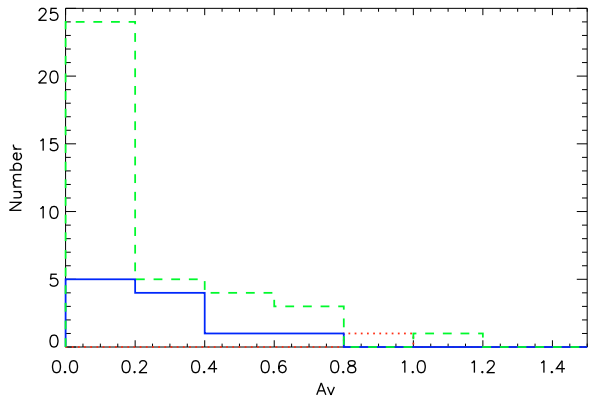

Fig. 8. Histogram with the optical (rest frame V-band) extinctions observed for the different GRB types. Each group is identified with the same line styles and colours as in Fig. 2.

described by Jakobsson et al. (2004), adding the data provided by Fynbo et al. (2009) and new values that can be found in Table 1. The small number of observed short bursts limits our analysis to only the intermediate and long populations.

From the histogram, we can see that the number of optically dark intermediate bursts is significantly lower (5 out of 30 or 17%) than the number of dark long bursts (26 out of 89 or 29%). Using only detections, the K-S test indicates that the probability of having the same distribution for intermediate and long bursts is 6.3%. However, we note that the number of limits to afterglow detections in the optical is significant and that this may affect our interpretation. If we perform the K-S test, assuming detection at the limit level we obtain a probability of 9.3%.

3.5. Optical extinction

The majority of the dust absorption seen in long bursts are most accurately described by Small Magellanic Cloud (SMC) extinction laws (Kann et al. 2006; Starling et al. 2007; Kann et al. 2010; Schady et al. 2007, 2010).

If we plot a histogram of the optical extinction as A_V in the rest frame (see Fig. 8, data have been taken from Kann et al. 2010, 2008), we find that the distribution for intermediate bursts is equivalent to what is found for long bursts ($\langle A_{V,\mathrm{int}} \rangle = 0.24$ with a standard deviation of 0.21, while for long bursts $\langle A_{V,\mathrm{long}} \rangle = 0.33$, with a standard deviation of 0.54). A K-S test assigns a probability of 61% to the hypothesis of equal distribution between intermediate and long bursts, implying no significant difference between the two groups.

3.6. X-ray hydrogen column density

The column densities used here are taken from the works of Evans et al. (2009) and Campana et al. (2010), which infer the hydrogen column density from the absorption of metals in the X-ray spectra. The values listed in those works already have the contribution of the Milky Way galaxy subtracted, so that we consider only the extragalactic contribution.

For the column densities, (see Fig. 9), we see that the average column density measured for intermediate bursts is again very similar to that of long bursts ($\langle \log(N_{\mathrm{H,int}}) \rangle = 21.5 \pm 0.5$ vs. $\langle N_{\mathrm{H,long}} \rangle = 21.7 \pm 0.5$). A K-S test assigns a probability to the hypothesis of equivalent distributions of 8.2%, implying no significant difference. We again disregard the short burst population in this analysis, as the number of good measurements is too small to derive conclusions.

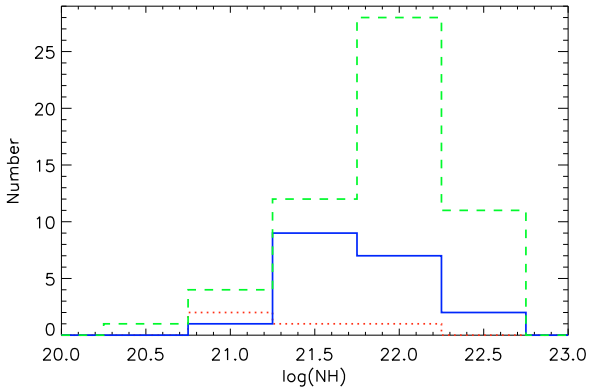

Fig. 9. Histogram with the hydrogen column density observed in the different GRB types as derived from X-ray observations. Each group is identified with the same line styles and colours as in Fig. 2.

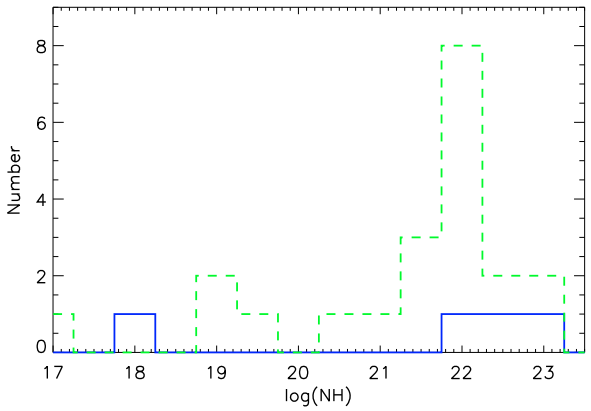

Fig. 10. Histogram with the hydrogen column density observed in the different GRB types, measured from Ly-α detections. Each group is identified with the same line styles and colours as in Fig. 2.

3.7. Optical hydrogen column density

We now consider at the hydrogen column density inferred directly from the fit to Ly-α absorption in optical spectra. This limits the sample to bursts that have redshifts higher than 2, when Ly-α starts to be detectable in the optical range. Figure 10 shows the distribution of the hydrogen column densities for long and intermediate bursts. Since there is no spectrum of a short burst within our sample, we exclude this group from this part of the analysis. For intermediate bursts, we have only 4 bursts, so the information derived from this analysis is very limited. We see from this plot that there are no significant differences between the long and intermediate bursts, both populations containing bursts with high and low column densities.

We now repeat the plot of optically derived column densities vs. X-ray derived column densities (see Fig. 11) presented by Campana et al. (2010, see also Watson et al. 2007). The region of low optical column densities with respect to X-ray ones is attributed by Campana et al. (2010) to the ionisation of material close to the progenitor. Detecting a trend for a particular type in this region of the diagram may be indicative of a difference in the burst environment. However, we see that there is no difference in the distribution of long or intermediate bursts with both types being present in all regions of the diagram but we note that the intermediate burst sample for this analysis consists of only four bursts.

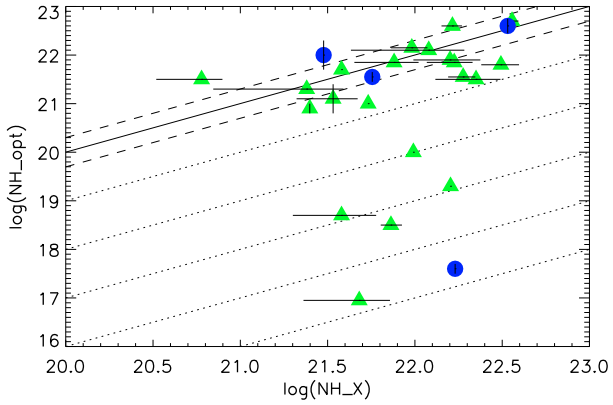

Fig. 11. X-ray column densities versus hydrogen column densities obtained from optical spectra. Dashed lines indicate values within a factor of 2 from the line of equal X-ray to optical column density (continuous line). Dotted lines mark optical column densities nth orders of magnitude less than X-ray ones. Each group is identified with the same symbols and colours as in Fig. 1.

3.8. Absorption line strength

Using the spectral data set compiled by Fynbo et al. (2009), we compare the spectra of the different GRB groups to search for differences in absorption line intensities. Unfortunately, the lack of short GRB spectra does not allow us to compare with short bursts, so the comparison is made only between long and intermediate bursts. To investigate whether there is any additional difference between long and intermediate bursts, we compare the rest-frame equivalent width (EW) distribution of several strong absorption features commonly detected in GRB spectra: C IIλ1535, C IVλ1549 (blended doublet in the sample), Si IIλ1526, and Si IVλ1393. The EW is related to the amount of material located in the line-of-sight of the GRB, larger EWs representing more material within the host galaxy. For the absorption lines, we chose two ionisation states of the same element to investigate a possible difference in the ionisation state of the material within the host galaxy. A strong trend in the ionisation state may be indicative of a different environment and/or progenitor, although the material observed in absorption has been shown to usually be located at large distances from the burst site (Vreeswijk et al. 2007; D'Elia et al. 2009).

In Fig. 12, we can see that the number of spectra of intermediate bursts remains very limited. This is not enough to enable us to perform reliable K-S tests. However, we can see that the values tend to agree with those of the long bursts, implying that the host environments of intermediate GRBs do not differ significantly from those of long bursts.

3.9. Supernova components

The clearest evidence linking long GRBs to the death of massive stars is the observation of a contemporaneous supernova event, as has been achieved spectroscopically in some events (Stanek et al. 2003; Hjorth et al. 2003; Malesani et al. 2004; Pian et al. 2006) and photometrically for larger samples (Galama et al. 1998; Zeh et al. 2004; Ferrero et al. 2006). On the other hand, all searches for supernova components in short bursts have failed to detect them, in some cases to very deep limits (Castro-Tirado et al. 2005; Hjorth et al. 2005a,b; Ferrero et al. 2007; Kann et al. 2008; Kocevski et al. 2010). This has been used to argue that short GRBs are produced by the coalescence of a compact binary system (Hjorth et al. 2005a).

Table 2. Supernova components for GRBs with redshift <1.0.

Short bursts			Intermediate bursts			Long bursts		
GRB	SN?	Reference	GRB	SN?	Reference	GRB	SN?	Reference
050509B	N	Hjorth et al. 2005a	050223	–	–	050826	–	–
050813	N	Ferrero et al. 2007	050416A	Y	Soderberg et al. 2007	060202	–	–
051221A	N	Soderberg et al. 2006	050525A	Y	Della Valle et al. 2006b	060218	Y	Pian et al. 2006
060502B	N	Kann et al. 2008	050724	N	Berger et al. 2005c	060602A	–	–
061006	–	–	050824	Y	Sollerman et al. 2007	060729	–	–
061201	N	Stratta et al. 2007	051016B	–	–	060814	–	–
061210	–	–	051109B	–	–	060904B	–	–
061217	–	–	060505	N	Fynbo et al. 2006	061021	–	–
070429B	–	–	060614	N	Fynbo et al. 2006	061028	–	–
070714B	–	–			Della Valle et al. 2006b	061110A	–	–
070724A	N	Kocevski et al. 2010			Gal-Yam et al. 2006	070318	–	–
070809	–	–	060912	–	–	070419A	Y	Dai et al. 2008
071227	N	D'Avanzo et al. 2009	071010A	Y	Covino et al. 2008	070508	–	–
080905A	N	Rowlinson et al. 2010	080430	–	–	070612A	–	–
			081007	Y	Della Valle et al. 2008	071010B	–	–
						080319B	Y	Tanvir et al. 2008 Bloom et al. 2009
						080710	–	–
						080916A	–	–
0 Yes	8 No	6 No data	5 Yes	3 No	5 No data	3 Yes	0 No	15 No data

Notes. For each group, we present three columns containing the name of the burst, the existence of a detected supernova (Y for yes; N for no; – if the data are not constraining), and references. The last row provides a summary of the total number for each case.

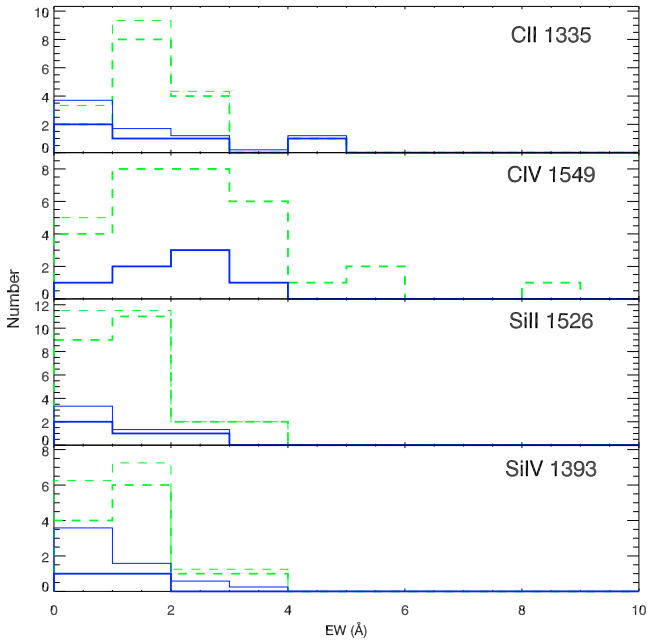

Fig. 12. Histogram with the rest-frame equivalent widths of several absorption features commonly observed in GRB afterglow spectra. Each group is identified with the same line styles and colours as in Fig. 2, where thick lines indicate detections and thin ones are detection limits.

When attempting a reliable and systematic study of the supernova components in a sample of GRBs, we encounter a number of problems. First, current instrumentation allows us to detect supernova components only for redshifts lower than ~1.0, with observations already becoming difficult at redshifts larger than 0.5. This limits the number of bursts for which these kind of studies are feasible, especially in the long burst sample. Furthermore, supernova component searches require a lot of telescope time as data for several epochs are needed to confirm the detection. Finally, the presence of a bright host galaxy complicates the detection of supernova bumps in the light curves.

Here we search for supernova components in the sample of bursts with redshifts lower than 1.0. Because of the different redshift distributions, we end up with 14 short bursts, 13 intermediate bursts, and 18 long bursts. The results are summarised in Table 2. Of the eight studies performed for short bursts, none of them detected a supernova component. For long bursts, there were only three detections of supernova components and 15 cases in which there is not enough observational data to reach definitive conclusions. For intermediate bursts, in five cases there was a supernova component detected and surprisingly, in three cases there was no supernova found. We note, however, that GRB 050724 is generally accepted to be a short burst (Berger et al. 2005c), probably being mistakenly identified as intermediate because of the intrinsic uncertainty in the method (see also Sect. 3.11). The origin of the other two bursts (GRB 060505 and GRB 060614) remains controversial: they have been argued to be linked to the explosions of massive stars that produce very little radioactive nickel and thus no radioactivity-driven SN emission (Fynbo et al. 2006; Della Valle et al. 2006a; Gal-Yam et al. 2006; Thöne et al. 2008; McBreen et al. 2008; Tominaga et al. 2007; Fryer et al. 2006, 2007), whereas other indicators point to an origin in merging compact objects despite their longer duration, which would naturally not be accompanied by SN emission (Gehrels et al. 2006; Zhang et al. 2007; Ofek et al. 2007; Kann et al. 2008; Krimm et al. 2009).

Since most intermediate bursts contain a supernova component, they probably share with long bursts an origin in collapsars. However, it is puzzling that there are cases where there has been no supernova detected for intermediate bursts.

3.10. Host galaxies

It has been shown that most long GRBs are hosted by star-forming galaxies (Christensen et al. 2004; Savaglio et al. 2009) and that they are generally located within the most active

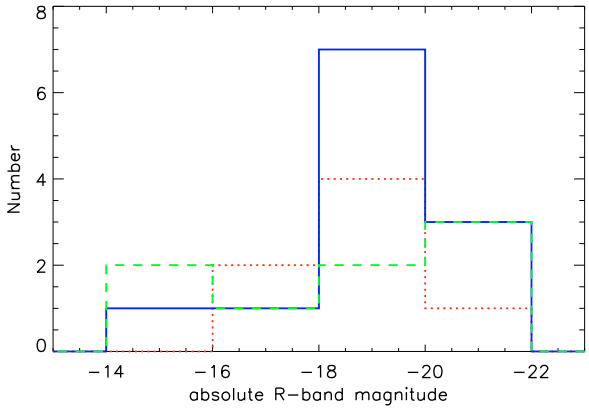

Fig. 13. Histogram with the absolute magnitudes of the host galaxies of the three GRB classes. Data have been taken from observed *R*-band magnitudes and include a rough k-correction. Each group is identified with the same line styles and colours as in Fig. 2.

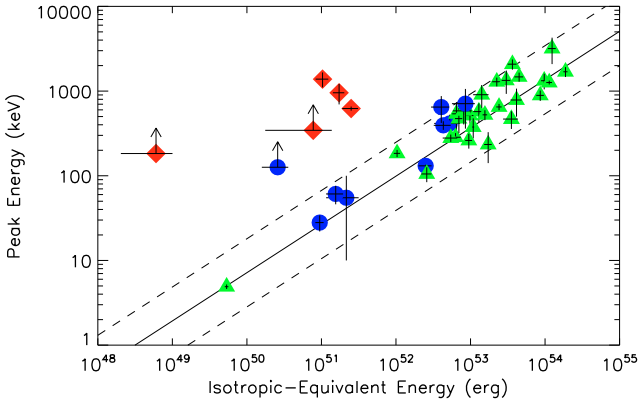

Fig. 14. Correlation between the peak energy and the isotropic-equivalent energy of the different types of GRBs. Each group is identified with the same symbols and colours as in Fig. 1.

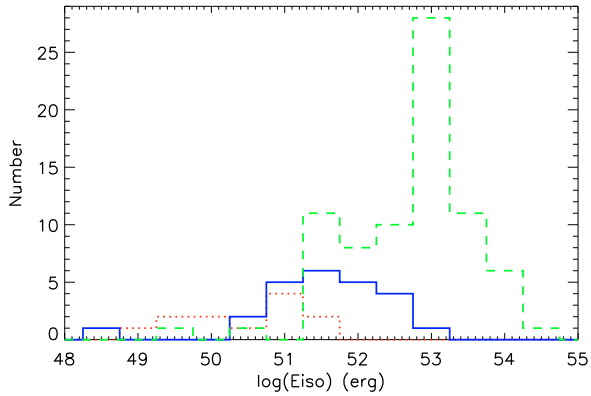

Fig. 15. Distribution of the $E_{\rm iso}$ measured for the different groups. Each group is identified with the same line styles and colours as in Fig. 2.

star-forming regions of these galaxies (Fruchter et al. 2006; Svensson et al. 2010). Short GRBs, on the other hand, are found in far more heterogeneous samples of galaxies (Berger 2009). In the present section, we study the characteristics of galaxies hosting intermediate bursts.

We compare the absolute magnitudes of all three classes using their observed *R*-band magnitudes. The sample of galaxies was taken from Savaglio et al. (2009), Perley et al. (2009), and Berger (2009). To derive the absolute magnitudes, we apply a rough k-correction assuming a spectral slope of −0.5.

There is no significant difference in the distribution of the absolute host magnitudes of the three classes (see Fig. 13). For the average and median of intermediate bursts, we find values of −19.9 and −20.3 mag with a dispersion of 1.5 mag. The values for short GRB hosts infer average and median values of −19.8 and −19.9 mag with a dispersion of 1.6 mag. A K-S test for short and intermediate bursts infers a 75% probability of being drawn from the same population. For long GRB hosts, we derive an average and median of −19.7 and −19.9 mag with a dispersion of 2.7. The K-S test for long and intermediate host magnitudes infer a probability of 41% that they are drawn from the same population, while for long and short hosts it is 25%. This implies that there is no significant difference in the luminosity of all three burst classes. We note, however, that the very small number of published data for GRB hosts in our sample (7 short, 12 intermediate, and 8 long) ensures that the comparison is unreliable. We are aware that comparing a parameter such as the star-forming rate, the metallicity, or the galaxy type would detect more significant differences in this kind of study where we intend to compare different environments but the amount of such data is even more scarce. A more thorough study will have to wait until more data on GRB host galaxies become available.

3.11. $E_{\rm peak}$ vs. $E_{\rm iso}$ correlation

To finalise our analysis of the characteristics of intermediate bursts in the *Swift* sample, we consider the prompt emission properties. We study first the correlation between the peak energy of the emission ($E_{\rm peak}$) and the isotropic energy release ($E_{\rm iso}$). It has been shown that this correlation is valid for long bursts but not for short bursts (Amati et al. 2002, 2008). In this section, we test where the different types of bursts within our sample fall in the $E_{\rm peak}$ vs. $E_{\rm iso}$ diagram.

Figure 14 shows that the distribution of intermediate GRBs follows reasonably well the $E_{\rm peak}$ vs. $E_{\rm iso}$ correlation. However, we do note a tendency of the intermediate bursts to lie above the correlation, in the region of lower $E_{\rm iso}$ or higher $E_{\rm peak}$ than the average long bursts. There is one intermediate burst that clearly lies outside the correlation. However, we note that this burst, GRB 050724, is generally accepted to be a short burst in the literature (Berger et al. 2005c) and its location on the $E_{\rm peak}$ vs. $E_{\rm iso}$ diagram has been discussed (Amati 2006), and postulated to probably be a misidentified short burst.

From the $E_{\rm peak}$ vs. $E_{\rm iso}$ diagram, we can also see that the intermediate bursts tend to have lower isotropic equivalent energies than long bursts. The distribution of $E_{\rm iso}$ (Fig. 15), where we have a larger sample, exhibits a clear difference in the distribution of the different types. A K-S test strongly rejects the hypothesis of equal distributions for short and long bursts, which has a probability of only 7.6×10^{-7}%, for short and intermediate infers a probability of 0.5%, and for intermediate and long of 0.0006%, which corresponds again to a strong rejection.

3.12. Spectral lags

In the second part of our analysis of the prompt characteristics of *Swift* bursts, we consider the spectral lags. The time profile of gamma-ray bursts appear to display high-energy band emission preceding the arrival of photons to low-energy bands.

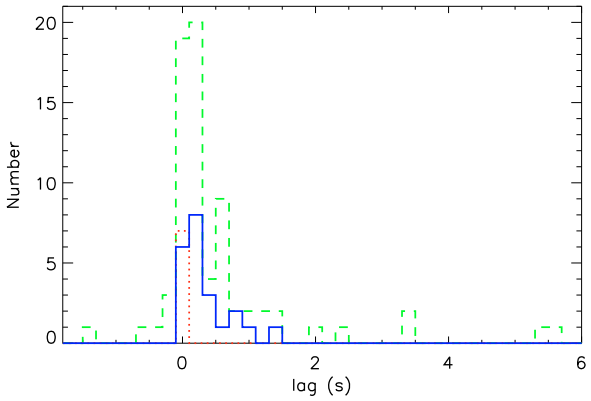

Fig. 16. Histogram showing the distribution of spectral lags of the different GRB types. Each group is identified with the same line styles and colours as in Fig. 2.

This observed lag between the bands is a direct consequence of the spectral evolution of GRBs, where the peak energy of the spectrum decays with time (Kocevski & Liang 2003; Gehrels et al. 2006; Norris & Bonnell 2006). It has been noted that the distribution of these lags is different for short and long bursts (Yi et al. 2006; Foley et al. 2009). In this section, we study the difference in the distribution of spectral lags of intermediate bursts and those of the other two populations. To do so, we use the sample published by Foley et al. (2009) completed for this work, as displayed in Table 1.

Figure 16 shows a clear tendency of the short bursts to have negligible lags (the median lag for short bursts is 6 ms with a standard deviation of 17 ms), while both intermediate and long bursts exhibit spectral lags, with a trend towards positive lags (the median lag for intermediate bursts is 250 ms with a standard deviation of 350 ms, while for long bursts it is 190 ms with a standard deviation of 1870 ms). A K-S test reveals that the probability of short and long bursts having the same distribution of lags is only 0.007%. For short and intermediate bursts, the probability is 0.004%, leading to an even stronger rejection. On the other hand, the probability of having the same distribution of lags in intermediate and long bursts is 76%, implying that there are no significant differences between them.

4. On the physical differences between intermediate and long bursts

In the previous sections, we have collected statistical data about a range of GRB properties to investigate whether a third group of intermediate bursts actually exists. It remains to be answered whether there is any physical motivation for the existence of this third group. Intermediate bursts appear to differ from short events, but they share many physical properties with long bursts (e.g., their environment and spectral properties are similar). To obtain some inference about the intrinsic differences between intermediate and long events we consider the set of the bursts in Table 1 for which $E_{\gamma,\rm iso}$ is known. GRB 060218 is excluded from this sample because of its atypical properties, which make it difficult to classify it as a standard long burst. This selection criterion yields 84 long bursts, 30 intermediate bursts, and only 14 short events. A number of average observational properties of these bursts (redshift z, duration T_{90}, intrinsic duration in the source frame $T'_{90} = T_{90}/(1+z)$, equivalent isotropic energy in gamma-rays, and peak energy $E_{\rm peak}$) and several estimated (γ-ray luminosity) or modeled properties (Lorentz factors) are listed in Table 3. The size of the sample of short bursts is obviously too small to infer good statistical properties. Hence, our inferences about these events have to be taken cautiously.

Table 3. Average values of some properties of the sample of events with known $E_{\gamma,\rm iso}$.

Properties	Short	Intermediate	Long
$\bar{z}$	0.5 ± 0.3	1.8 ± 1.5	2.2 ± 1.3
$\bar{T}_{90}$	0.6 ± 0.5	10 ± 6	110 ± 110
$\bar{T}'_{90}$	0.4 ± 0.4	4 ± 4	40 ± 40
$\bar{E}_{\gamma,\rm iso}$	50.4 ± 0.9	51.6 ± 1.0	52.7 ± 0.8
$\bar{E}_{\rm peak}$	90 ± 180	200 ± 300	300 ± 500
$\bar{L}_{\gamma,\rm iso}$	50.7 ± 0.9	50.7 ± 1.0	50.8 ± 0.8
$\bar{L}'_{\gamma,\rm iso}$	50.9 ± 0.9	51.1 ± 1.2	51.3 ± 0.9
$\bar{\Gamma}_{\rm thk}$	2000 ± 800	1200 ± 500	700 ± 300
$\bar{\Gamma}_{\rm thn}$	700 ± 300	420 ± 190	150 ± 60

Notes. The first five columns display averages of observed properties: $\bar{z}$ is the average redshift, $\bar{T}_{90}$ is the average duration, $\bar{T}'_{90}$ is the average intrinsic burst duration ($T'_{90} = T_{90}/(1+z)$), $\bar{E}_{\gamma,\rm iso}$ is the average of $\log(E_{\gamma,\rm iso})$, and $\bar{E}_{\rm peak}$ is the average peak energy. The next two rows correspond to values readily computed from the observed ones: $\bar{L}_{\gamma,\rm iso}$ is the average of $\log(L_{\gamma,\rm iso}) = \log(E_{\rm iso}/T_{90})$, and $\bar{L}'_{\gamma,\rm iso}$ is the average of $\log(L'_{\gamma,\rm iso}) = \log(E_{\gamma,\rm iso}/T'_{90})$. The final two rows display different estimates of the Lorentz factor of the ejecta assuming that the external medium density is $n_{\rm ext} = 10$ cm^{-3} and that it is either thick ($\Gamma_{\rm thk}$; $\xi = 0.35$) or thin ($\Gamma_{\rm thn}$; $\xi = 3$).

A simple inspection of the first five rows of Table 3 shows that the redshift distribution of long and intermediate events is basically the same, while short bursts are clearly closer to us. The average duration (either observed or intrinsic) of long bursts is ∼10 times larger than that of intermediate ones. Despite both long and intermediate events following Amati's relation (Sect. 3.11), both the average $E_{\gamma,\rm iso}$ and $E_{\rm peak}$ are lower for intermediate events than for long bursts (but still, are approximately the same within the statistical errors). All families of bursts have a similar *observed* γ-luminosity, but the *intrinsic* luminosity of long and intermediate burst appears to be somewhat higher than that of short bursts. The similarity between the observed luminosity, but different intrinsic duration and $E_{\gamma,\rm iso}$ might be used to infer differences in the expected bulk Lorentz factor of the ejecta. We obtain two different estimates of the bulk Lorentz factor, in both the cases assuming an external medium number density $n_{\rm ext} = 10$ cm^{-3} and a efficiency of conversion of the total ejecta energy E to γ-rays of $\eta := E_{\gamma,\rm iso}/E = 0.2$ (Mimica & Aloy 2010). We compute the Lorentz factor using the dimensionless variable $\xi = (l/\Delta)^{1/2}\Gamma^{-4/3}$ (Sari & Piran 1995) that controls whether the ejecta is either thin ($\xi > 1$) or thick ($\xi < 1$). For thick (thin) ejecta, we take $\xi = 0.35$ ($\xi = 3$), and obtain the value $\Gamma_{\rm thk}$ ($\Gamma_{\rm thn}$) for each burst, which yields the average values listed in the last two rows of Table 3. It is clear that the average values tend to increase with decreasing burst duration, such that intermediate GRBs exhibit larger bulk Lorentz factors than long events, regardless of whether we consider the ejecta to be in the thin or thick shell regime. However, the standard deviation and small sample size do not allow a definitive conclusion to be drawn. We note that if short and intermediate events originate in thin shells, they may have, on average, smaller bulk Lorenz factors than long bursts (compare $\Gamma_{\rm thk}$ for long events with $\Gamma_{\rm thn}$ for short and intermediate events in Table 3). That short events

display even larger bulk Lorentz factors than intermediate events (in cases where they are both produced by thin shells) is consistent with the results of earlier numerical simulations (e.g., Aloy et al. 2005), which adds some confidence to the trend found here (that in the case of short events is affected by the small size of the sample).

We can improve our analysis by checking whether the bulk Lorentz factor estimated for each burst is bounded by the minimum Lorentz factor $\Gamma_{\rm min}$ to overcome the compactness problem and the maximum Lorentz factor $\Gamma_{\rm max}$ to prevent electrons and protons becoming decoupled in the ejecta (see, e.g., Waxman 2003). In Fig. 17, we highlight bursts for which the estimated bulk Lorentz factor falls between the allowed range for different choices of the parameters ξ and $n_{\rm ext}$. Long bursts are hard to accommodate if the ejecta are thin (note that they are not highlighted in the upper panels). The reason for this is that the estimated Lorentz factor is too small to overcome the compactness restriction. Likewise, short bursts seem difficult to fit if the ejecta are thick. In this case, the inferred Lorentz factors are too large (i.e., possibility of short bursts being produced in thick shells is excluded because $\Gamma > \Gamma_{\rm max}$). The case of intermediate bursts is not so clear, but most of them possess bulk Lorentz factors in the permitted range if the ejecta are thin shells. Indeed, nearly all intermediate events are properly parametrized by thin shells if we consider a more dilute external medium ($n_{\rm ext} = 1$ cm^{-3}; Fig. 17, lower graph of top panel) than in our reference case (with $n_{\rm ext} = 10$ cm^{-3}).

These results suggest that the main physical difference between intermediate and long bursts is that for intermediate bursts (and probably also in the case of short events) the ejecta are thin shells, while for long bursts ejecta are typically thick. This interpretation accounts also for the shorter duration of intermediate bursts relative to long ones, since the ejecta thickness is $\Delta \sim cT'_{90}$ (Table 3).

Although there are no statistical indications that long and intermediate events were produced in different environments (see Sects. 3.6 and 3.7), it is remarkable that the combination of both thin shell ejecta and relatively low circumburst density, optimally accommodates the estimated Lorentz factor of intermediate bursts. However, we point out that the estimated bulk Lorentz factor depends very slightly on the circumburst medium number density ($\Gamma_{\rm thk,thn} \propto n_{\rm ext}^{-1/8}$).

Our aforementioned results support the hypothesis that intermediate and long bursts probably have the same progenitors. The intrinsic shorter duration of the former events suggests that either the central engine is active for a shorter time than in long bursts or that the efficiency of the energy extraction is lower than in long events. A short-lived central engine may be produced by a thermally driven relativistic outflow (Aloy & Obergaulinger 2007; Nagataki et al. 2007), or perhaps the magnetic flux in the vicinity of the outflow being only slightly above the critical value to activate the Blandford-Znajek mechanism (e.g., Komissarov & Barkov 2009). If the type-defining property of intermediate bursts were the magnetic field strength, an additional means of distinguishing the properties of their central engines would be provided by the early optical afterglow observations. The absence of a reverse shock signature may be indicative of ejecta magnetization $\sigma > 0.1$ (Mimica et al. 2009, 2010). Unfortunately, most of the optical observations analyzed in this paper did not capture the GRB afterglow early enough to make use of this property in the characterization of intermediate bursts. Thus, with the available data it is hardly possible to make more than educated inferences about the properties that differentiate between the central engines of intermediate and long bursts.

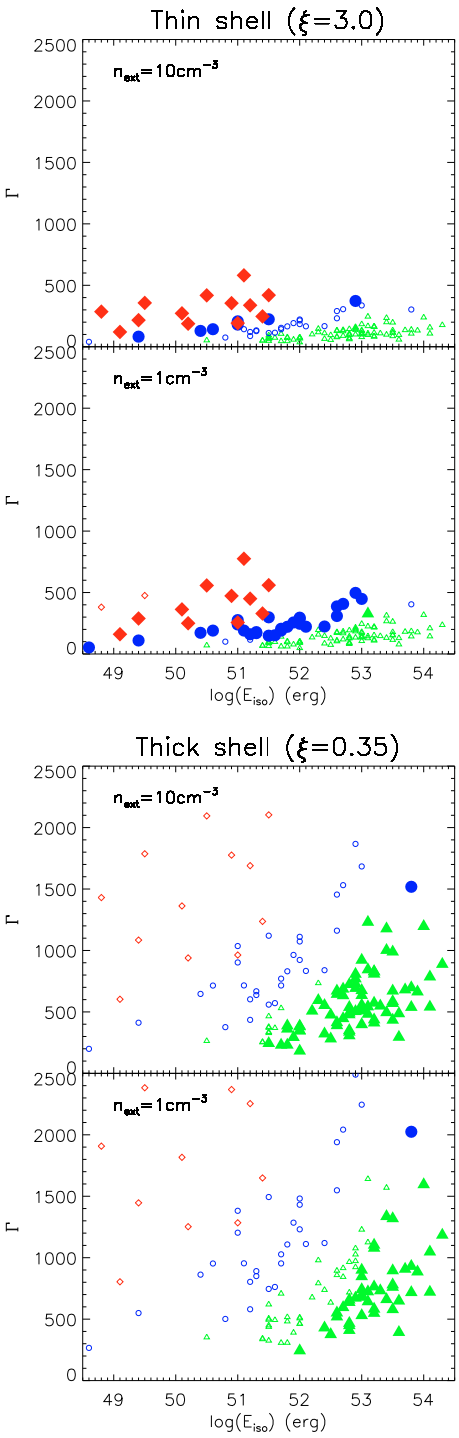

Fig. 17. Estimated bulk Lorentz factor for the sample of burst with known $E_{\gamma,\rm iso}$. In *the top panels*, we assume a value of the dimensionless ξ parameter typical of ejecta in the so-called thin shell regime. In *the bottom panels*, we consider $\xi = 0.35$, a typical value for thick shells. In the upper (lower) subpanels, we assume an external medium particle density of $n_{\rm ext} = 10$ cm^{-3} ($n_{\rm ext} = 1$ cm^{-3}). Red diamonds, blue circles, and green triangles correspond to short, intermediate, and long events, respectively. Only the bursts represented with bigger filled symbols possess a Lorentz factor in the allowed range $[\Gamma_{\rm min}, \Gamma_{\rm max}]$ (see text).

5. Discussion and conclusions

We have analysed the sample of the first four years of *Swift* bursts divided into three groups as described by Horváth et al. (2010). We have defined the characteristics of the intermediate

Table 4. Summary of the K-S test results.

Parameter	Short-Long	Short-Int	Int.-Long
Redshift	9.5×10^{-5} **%**	**0.15%**	14%
Lum. $X_{10^2\ s}$	**0.02%**	1.6%	**0.005%**
Lum. $X_{10^4\ s}$	**0.002%**	**0.08%**	**0.007%**
Mag. $O_{10^2\ s}$	–	–	11%
Mag. $O_{10^4\ s}$	–	–	3.3%
Dark bursts	–	–	6.3%
Extinction	–	–	[61%]
$N_{H,X}$	–	–	8.2%
Spec. lags	**0.018%**	**0.009%**	[76%]
Host galaxies	25%	[75%]	[41%]
E_{iso}	8×10^{-7} **%**	**0.5%**	**0.0006%**

Notes. Bold font indicates the results that show conclusive evidence of difference (<1%) and brackets those results that provide evidence of strong similarities (>30%).

Table 5. Median and standard deviation of parameters used in the comparison.

Parameter	Short	Intermediate	Long
Redshift	0.44 ± 0.31	1.55 ± 1.53	1.97 ± 1.33
log(Lum. $X)_{10^2\ s}$ (erg/s)	47.2 ± 0.6	47.9 ± 0.6	49.1 ± 1.6
log(Lum. $X)_{10^4\ s}$ (erg/s)	44.4 ± 0.8	46.0 ± 0.7	46.7 ± 0.7
Mag. O 10^2 s	–	15.6 ± 2.0	13.8 ± 2.9
Mag. O 10^4 s	–	19.8 ± 2.3	18.1 ± 1.4
β_{OX}	–	0.91 ± 0.15	0.74 ± 0.21
A_V	–	0.21 ± 0.21	0.16 ± 0.54
log($N_{H,X}$) (cm^{-2})	–	21.5 ± 0.5	21.7 ± 0.5
Spectral lags (ms)	6 ± 17	250 ± 350	190 ± 1870
log(E_{iso}) (erg)	50.9 ± 0.9	51.6 ± 0.9	52.9 ± 0.9

class and searched for differences in a range of properties compared to the other two, well established groups. The contamination of the two other groups in the intermediate region of the HR vs. T_{90} diagram motivated an analysis on possible differences in the statistical sample, because conclusions based on individual bursts can be misleading. Tables 4 and 5 summarise the results of the K-S comparison tests of several properties between groups and the median values of several parameters.

We note that the classification method used in this paper is based on observer frame properties of the burst. A detailed rest-frame classification has not yet been performed in a reliable way, because of the limited number of bursts with measured redshift. This classification would allow us to derive intrinsic properties and would be more physically significant.

The statistically most significant difference between the three groups is the distribution of their energetics and afterglow luminosities. Intermediate bursts exhibit a clear difference in luminosity of the afterglows with respect to the short and long types, with intermediate bursts being brighter than short bursts and dimmer than long bursts. This difference is clearly observed in X-ray light curves, where the measured luminosity for intermediate bursts is on average one order of magnitude fainter than long bursts and one order of magnitude brighter than short bursts, but less significant in the optical.

To a smaller extent, there seems to be a trend in the redshift distribution of the three groups. We find that intermediate bursts are, on average, closer than long bursts and further away than short bursts. The difference between short bursts and the other two types is statistically significant, but any differences between intermediate and long bursts are smaller. An analysis of a significantly larger number of events will be needed in order to confirm this trend.

Looking at the burst environment, there seems to be no clear distinction between long and intermediate bursts leaving us with the conclusion that their environments are not largely different. Short bursts have to be disregarded in these studies due to the lack of data. There is no clear difference between intermediate and long bursts in terms of the hydrogen column densities derived from both optical and X-rays. Likewise, no difference is found in either the optical extinction or in the absorption line strength measured in optical spectra. The data on host galaxies of GRBs within our sample is very limited. A comparison of the absolute magnitudes of the different types does not show any significant difference in any of the different groups. A study of more significant parameters, such as metallicity, star formation rate or galaxy type is not possible at this time due to the lack of data.

An important indicator of the nature of the progenitor of the three groups would be the detection or non-detection of a SN in the afterglow or spectra of the GRB. However, for observational reasons, this is limited to bursts below redshift ∼1. Also here, the sample of GRBs with searches or detections of SN components is too small to make any firm conclusion. While short bursts do not exhibit any evidence of a SN despite a number of searches and the long burst sample contains only three bursts with SN searches, intermediate bursts contain both SN detections and non-detections. Of the three non-detections, one burst is usually classified as short, while the other two have proven to be controversial bursts, i.e. GRB 060505 and GRB 060614.

Finally, we have compared the prompt emission properties of the different samples. Intermediate bursts follow the E_{peak} vs. E_{iso} correlation described by Amati et al. (2002), as the long bursts do, while short bursts always lie outside of it. We note a slight trend of intermediate bursts lying above the correlation. Finally, a study of the spectral lags observed in the prompt emission of the GRBs shows that intermediate bursts behave similarly to long bursts, with mainly positive lags and are clearly different from short bursts, which show negligible lags.

We suggest that the physical difference between intermediate and long bursts is that in the former case, the ejecta are thin shells, while in the latter they are thick shells. This would also explain why the durations of intermediate bursts are shorter than those of long bursts. Apart from this, intermediate and long bursts appear to have the same type of progenitors.

Summarizing the results on the three groups, there is some evidence that intermediate and long bursts differ in termsof their afterglow luminosity and prompt emission properties, while short bursts are clearly a distinct group. Intermediate and long GRBs, however, do not seem to reside in different environments and their progenitors might be rather similar, hence both coming from a collapsar but with subtle differences leading to a lower afterglow luminosity and shorter duration for the intermediate class. For most properties, the lack of sufficient data does not allow a proper analysis of the statistical significance of the differences between the three groups. Thus, a future study with a significantly larger sample might be capable of drawing more precise conclusions.

Acknowledgements. This work is supported by ASI grant SWIFT I/011/07/0, of the Ministry of University and Research of Italy (PRIN MIUR 2007TNYZXL), by AYA 2009-14000-C03-01, from the spanish Ministry of Science and Innovation, by AYA2007-67626-C03-01, from the Spanish Ministry of Science and Innovation, by PROMETEO/2009/103 from the Valencian Conselleria

d'Educació, by OTKA K077795, by OTKA/NKTH A08-77719 and by A08-77815. A.d.U.P. acknowledges support from an ESO fellowship. IH acknowledges support from a Bolyai Scholarship. S.F. acknowledges the support of the Irish Research Council for Science, Engineering and Technology, cofunded by Marie Curie Actions under FP7. M.A.A. gratefully acknowledges the enlightening discussions with Petar Mimica.

References

Akerlof, C., Balsano, R., Barthelmy, S., et al. 1999, Nature, 398, 400
Aloy, M. A., & Obergaulinger, M. 2007, Rev. Mex. Astron. Astrofis. Conf. Ser., 30, 96
Aloy, M. A., Janka, H., & Müller, E. 2005, A&A, 436, 273
Amati, L. 2006, Nuovo Cimento B Serie, 121, 1081
Amati, L., Frontera, F., Tavani, M., et al. 2002, A&A, 390, 81
Amati, L., Guidorzi, C., Frontera, F., et al. 2008, MNRAS, 391, 577
Barthelmy, S. D., Chincarini, G., Burrows, D. N., et al. 2005, Nature, 438, 994
Berger, E. 2006, GRB Coordinates Network, 5962, 1
Berger, E. 2009, ApJ, 690, 231
Berger, E., & Becker, G. 2005, GRB Coordinates Network, 3520, 1
Berger, E., & Rauch, M. 2008, GRB Coordinates Network, 8542, 1
Berger, E., Fox, D. B., Kulkarni, S. R., et al. 2005a, ApJ, 629, 328
Berger, E., Kulkarni, S. R., Fox, D. B., et al. 2005b, ApJ, 634, 501
Berger, E., Price, P. A., Cenko, S. B., et al. 2005c, Nature, 438, 988
Berger, E., Kulkarni, S. R., Rau, A., & Fox, D. B. 2006a, GRB Coordinates Network, 4815, 1
Berger, E., Penprase, B. E., Cenko, S. B., et al. 2006b, ApJ, 642, 979
Berger, E., Fox, D. B., & Cucchiara, A. 2007a, GRB Coordinates Network, 6470, 1
Berger, E., Fox, D. B., Price, P. A., et al. 2007b, ApJ, 664, 1000
Berger, E., Foley, R., Simcoe, R., & Irwin, J. 2008a, GRB Coordinates Network, 8434, 1
Berger, E., Fox, D. B., Cucchiara, A., & Cenko, S. B. 2008b, GRB Coordinates Network, 8335, 1
Bloom, J. S., Prochaska, J. X., Pooley, D., et al. 2006, ApJ, 638, 354
Bloom, J. S., Perley, D. A., Chen, H., et al. 2007, ApJ, 654, 878
Bloom, J. S., Perley, D. A., Li, W., et al. 2009, ApJ, 691, 723
Boër, M., Atteia, J. L., Damerdji, Y., et al. 2006, ApJ, 638, L71
Butler, N. R. 2007, ApJ, 656, 1001
Campana, S., Thöne, C. C., de Ugarte Postigo, A., et al. 2010, MNRAS, 402, 2429
Castro-Tirado, A. J., & Gorosabel, J. 1999, A&AS, 138, 449
Castro-Tirado, A. J., de Ugarte Postigo, A., Gorosabel, J., et al. 2005, A&A, 439, L15
Cenko, S. B., Berger, E., Djorgovski, S. G., Mahabal, A. A., & Fox, D. B. 2006, GRB Coordinates Network, 5155, 1
Cenko, S. B., Cucchiara, A., Fox, D. B., Berger, E., & Price, P. A. 2007a, GRB Coordinates Network, 6888, 1
Cenko, S. B., Fox, D. B., Cucchiara, A., et al. 2007b, GRB Coordinates Network, 6556, 1
Cenko, S. B., Berger, E., Nakar, E., et al. 2008, [arXiv:0802.0874]
Chattopadhyay, T., Misra, R., Chattopadhyay, A. K., & Naskar, M. 2007, ApJ, 667, 1017
Christensen, L., Hjorth, J., & Gorosabel, J. 2004, A&A, 425, 913
Covino, S., D'Avanzo, P., Klotz, A., et al. 2008, MNRAS, 388, 347
Cucchiara, A., Fox, D. B., & Cenko, S. B. 2007a, GRB Coordinates Network, 7124, 1
Cucchiara, A., Fox, D. B., Cenko, S. B., & Price, P. A. 2007b, GRB Coordinates Network, 6083, 1
Dai, X., Garnavich, P. M., Prieto, J. L., et al. 2008, ApJ, 682, L77
Daigne, F., & Mochkovitch, R. 1998, MNRAS, 296, 275
D'Avanzo, P., D'Elia, V., & Covino, S. 2008, GRB Coordinates Network, 8350, 1
D'Avanzo, P., Malesani, D., Covino, S., et al. 2009, A&A, 498, 711
de Ugarte Postigo, A., Christensen, L., Gorosabel, J., et al. 2008, GRB Coordinates Network, 7650, 1
D'Elia, V., Covino, S., & D'Avanzo, P. 2008a, GRB Coordinates Network, 8438, 1
D'Elia, V., Thoene, C. C., de Ugarte Postigo, A., et al. 2008b, GRB Coordinates Network, 8531, 1
D'Elia, V., Fiore, F., Perna, R., et al. 2009, ApJ, 694, 332
Della Valle, M., Chincarini, G., Panagia, N., et al. 2006a, Nature, 444, 1050
Della Valle, M., Malesani, D., Bloom, J. S., et al. 2006b, ApJ, 642, L103
Della Valle, M., Benetti, S., Mazzali, P., et al. 2008, Central Bureau Electronic Telegrams, 1602, 1
Evans, P. A., Beardmore, A. P., Page, K. L., et al. 2007, A&A, 469, 379
Evans, P. A., Beardmore, A. P., Page, K. L., et al. 2009, MNRAS, 397, 1177
Ferrero, P., Kann, D. A., Zeh, A., et al. 2006, A&A, 457, 857
Ferrero, P., Sanchez, S. F., Kann, D. A., et al. 2007, AJ, 134, 2118
Ferrero, P., Klose, S., Kann, D. A., et al. 2009, A&A, 497, 729
Foley, S., McBreen, S., McGlynn, S., McBreen, B., & Hanlon, L. 2009, in American Institute of Physics Conference Series, ed. C. Meegan, C. Kouveliotou, & N. Gehrels, AIP Conf. Ser., 1133, 403
Fong, W., Berger, E., & Fox, D. B. 2010, ApJ, 708, 9
Fruchter, A. S., Levan, A. J., Strolger, L., et al. 2006, Nature, 441, 463
Fryer, C. L., Young, P. A., & Hungerford, A. L. 2006, ApJ, 650, 1028
Fryer, C. L., Hungerford, A. L., & Young, P. A. 2007, ApJ, 662, L55
Fynbo, J. P. U., Watson, D., Thöne, C. C., et al. 2006, Nature, 444, 1047
Fynbo, J. P. U., Jakobsson, P., Prochaska, J. X., et al. 2009, ApJS, 185, 526
Gal-Yam, A., Fox, D. B., Price, P. A., et al. 2006, Nature, 444, 1053
Galama, T. J., Vreeswijk, P. M., van Paradijs, J., et al. 1998, Nature, 395, 670
Gehrels, N., Chincarini, G., Giommi, P., et al. 2004, ApJ, 611, 1005
Gehrels, N., Sarazin, C. L., O'Brien, P. T., et al. 2005, Nature, 437, 851
Gehrels, N., Norris, J. P., Barthelmy, S. D., et al. 2006, Nature, 444, 1044
Gehrels, N., Barthelmy, S. D., Burrows, D. N., et al. 2008, ApJ, 689, 1161
Ghisellini, G., Nardini, M., Ghirlanda, G., & Celotti, A. 2009, MNRAS, 393, 253
Greiner, J., Krühler, T., McBreen, S., et al. 2009, ApJ, 693, 1912
Hjorth, J., Sollerman, J., Møller, P., et al. 2003, Nature, 423, 847
Hjorth, J., Sollerman, J., Gorosabel, J., et al. 2005a, ApJ, 630, L117
Hjorth, J., Watson, D., Fynbo, J. P. U., et al. 2005b, Nature, 437, 859
Horváth, I. 1998, ApJ, 508, 757
Horváth, I. 2002, A&A, 392, 791
Horváth, I. 2009, Ap&SS, 323, 83
Horváth, I., Bagoly, Z., Balázs, L. G., et al. 2010, ApJ, 713, 552
Jakobsson, P., Hjorth, J., Fynbo, J. P. U., et al. 2004, ApJ, 617, L21
Jakobsson, P., Levan, A., Chapman, R., et al. 2006a, GRB Coordinates Network, 5617, 1
Jakobsson, P., Levan, A., Fynbo, J. P. U., et al. 2006b, A&A, 447, 897
Jakobsson, P., Malesani, D., Fynbo, J. P. U., et al. 2007, GRB Coordinates Network, 6997, 1
Jelínek, M., Prouza, M., Kubánek, P., et al. 2006, A&A, 454, L119
Kann, D. A., Klose, S., & Zeh, A. 2006, ApJ, 641, 993
Kann, D. A., Masetti, N., & Klose, S. 2007, AJ, 133, 1187
Kann, D. A., Klose, S., Zhang, B., et al. 2008, [arXiv:0804.1959]
Kann, D. A., Klose, S., Zhang, B., et al. 2010, ApJ, 720, 1513
Kawai, N., Kosugi, G., Aoki, K., et al. 2006, Nature, 440, 184
King, A., Olsson, E., & Davies, M. B. 2007, MNRAS, 374, L34
Kocevski, D., & Butler, N. 2008, ApJ, 680, 531
Kocevski, D., & Liang, E. 2003, ApJ, 594, 385
Kocevski, D., Thöne, C. C., Ramirez-Ruiz, E., et al. 2010, MNRAS, 404, 963
Komissarov, S. S., & Barkov, M. V. 2009, MNRAS, 397, 1153
Kouveliotou, C., Meegan, C. A., Fishman, G. J., et al. 1993, ApJ, 413, L101
Krimm, H. A., Yamaoka, K., Sugita, S., et al. 2009, ApJ, 704, 1405
Kuin, N. P. M., Landsman, W., Page, M. J., et al. 2009, MNRAS, 395, L21
Levan, A. J., Wynn, G. A., Chapman, R., et al. 2006, MNRAS, 368, L1
Lyutikov, M. 2009, [arXiv:0911.0349]
Malesani, D., Tagliaferri, G., Chincarini, G., et al. 2004, ApJ, 609, L5
Mazets, E. P., Golenetskii, S. V., Ilinskii, V. N., et al. 1981, Ap&SS, 80, 3
McBreen, S., Foley, S., Watson, D., et al. 2008, ApJ, 677, L85
Mészáros, A., Bagoly, Z., Horváth, I., Balázs, L. G., & Vavrek, R. 2000, ApJ, 539, 98
Mimica, P., & Aloy, M. A. 2010, MNRAS, 401, 525
Mimica, P., Giannios, D., & Aloy, M. A. 2009, A&A, 494, 879
Mimica, P., Giannios, D., & Aloy, M. A. 2010, MNRAS, 407, 2501
Mirabal, N., Halpern, J. P., & O'Brien, P. T. 2007, ApJ, 661, L127
Mukherjee, S., Feigelson, E. D., Jogesh Babu, G., et al. 1998, ApJ, 508, 314
Nagataki, S., Takahashi, R., Mizuta, A., & Takiwaki, T. 2007, ApJ, 659, 512
Narayan, R., Paczynski, B., & Piran, T. 1992, ApJ, 395, L83
Norris, J. P., & Bonnell, J. T. 2006, ApJ, 643, 266
Norris, J. P., Cline, T. L., Desai, U. D., & Teegarden, B. J. 1984, Nature, 308, 434
Norris, J. P., Gehrels, N., & Scargle, J. D. 2010, ApJ, 717, 411
Nysewander, M., Fruchter, A. S., & Pe'er, A. 2009, ApJ, 701, 824
Ofek, E. O., Cenko, S. B., Gal-Yam, A., et al. 2007, ApJ, 662, 1129
Paczynski, B. 1990, ApJ, 363, 218
Paczyński, B. 1998, in Gamma-Ray Bursts, 4th Hunstville Symposium, ed. C. A. Meegan, R. D. Preece, & T. M. Koshut, AIP Conf. Ser., 428, 783
Pellizza, L. J., Duc, P., Le Floc'h, E., et al. 2006, A&A, 459, L5
Penprase, B. E., Berger, E., Fox, D. B., et al. 2006, ApJ, 646, 358
Perley, D., & Kemper, Y. 2008, in American Institute of Physics Conference Series, ed. M. Galassi, D. Palmer, & E. Fenimore, AIP Conf. Ser., 1000, 631
Perley, D. A., Foley, R. J., Bloom, J. S., & Butler, N. R. 2006, GRB Coordinates Network, 5387, 1
Perley, D. A., Bloom, J. S., Butler, N. R., et al. 2008a, ApJ, 672, 449

Perley, D. A., Bloom, J. S., Modjaz, M., et al. 2008b, GRB Coordinates Network, 7889, 1
Perley, D. A., Li, W., Chornock, R., et al. 2008c, ApJ, 688, 470
Perley, D. A., Cenko, S. B., Bloom, J. S., et al. 2009, AJ, 138, 1690
Pian, E., Mazzali, P. A., Masetti, N., et al. 2006, Nature, 442, 1011
Price, P. A., Songaila, A., Cowie, L. L., et al. 2007, ApJ, 663, L57
Prochaska, J. X., Bloom, J. S., Chen, H., et al. 2006a, ApJ, 642, 989
Prochaska, J. X., Chen, H., Bloom, J. S., Falco, E., & Dupree, A. K. 2006b, GRB Coordinates Network, 5002, 1
Prochaska, J. X., Perley, D. A., Modjaz, M., et al. 2007, GRB Coordinates Network, 6864, 1
Quimby, R., Fox, D., Hoeflich, P., Roman, B., & Wheeler, J. C. 2005, GRB Coordinates Network, 4221, 1
Racusin, J. L., Karpov, S. V., Sokolowski, M., et al. 2008, Nature, 455, 183
Rees, M. J., & Meszaros, P. 1992, MNRAS, 258, 41P
Rowlinson, A., Wiersema, K., Levan, A. J., et al. 2010, MNRAS, 408, 383
Sari, R., & Piran, T. 1995, ApJ, 455, L143
Sari, R., Piran, T., & Halpern, J. P. 1999, ApJ, 519, L17
Savaglio, S., Glazebrook, K., & Le Borgne, D. 2009, ApJ, 691, 182
Schady, P., Mason, K. O., Page, M. J., et al. 2007, MNRAS, 377, 273
Schady, P., Page, M. J., Oates, S. R., et al. 2010, MNRAS, 401, 2773
Soderberg, A. M., Berger, E., & Ofek, E. 2005, GRB Coordinates Network, 4186, 1
Soderberg, A. M., Berger, E., Kasliwal, M., et al. 2006, ApJ, 650, 261
Soderberg, A. M., Nakar, E., Cenko, S. B., et al. 2007, ApJ, 661, 982
Sollerman, J., Fynbo, J. P. U., Gorosabel, J., et al. 2007, A&A, 466, 839
Stanek, K. Z., Matheson, T., Garnavich, P. M., et al. 2003, ApJ, 591, L17
Starling, R. L. C., Wijers, R. A. M. J., Wiersema, K., et al. 2007, ApJ, 661, 787
Stratta, G., D'Avanzo, P., Piranomonte, S., et al. 2007, A&A, 474, 827
Svensson, K. M., Levan, A. J., Tanvir, N. R., Fruchter, A. S., & Strolger, L. 2010, MNRAS, 405, 57
Tanvir, N. R., Rol, E., Levan, A., et al. 2008, ApJ, 725, 625
Thöne, C. C., Perley, D. A., & Bloom, J. S. 2007a, GRB Coordinates Network, 6663, 1
Thöne, C. C., Perley, D. A., Cooke, J., et al. 2007b, GRB Coordinates Network, 6741, 1
Thöne, C. C., Fynbo, J. P. U., Östlin, G., et al. 2008, ApJ, 676, 1151
Tominaga, N., Maeda, K., Umeda, H., et al. 2007, ApJ, 657, L77
Řípa, J., Mészáros, A., Wigger, C., et al. 2009, A&A, 498, 399
Vavrek, R., Balázs, L. G., Mészáros, A., Horváth, I., & Bagoly, Z. 2008, MNRAS, 391, 1741
Vreeswijk, P. M., Ledoux, C., Smette, A., et al. 2007, A&A, 468, 83
Watson, D., Hjorth, J., Fynbo, J. P. U., et al. 2007, ApJ, 660, L101
Waxman, E. 2003, in Lecture Notes in Physics, Supernovae and Gamma-Ray Bursters (Berlin: Springer Verlag), ed. K. Weiler, 598, 393
Woosley, S. E. 1993, ApJ, 405, 273
Yi, T., Liang, E., Qin, Y., & Lu, R. 2006, MNRAS, 367, 1751
Zeh, A., Klose, S., & Hartmann, D. H. 2004, ApJ, 609, 952
Zhang, B., Zhang, B., Liang, E., et al. 2007, ApJ, 655, L25

Table 1. Characteristics of *Swift* GRBs with known redshifts detected during the first four years of operations of the satellite.

GRB	T_{90} (s)	HR	P1	P2	P3	Type	z	$N_{\rm H,X}$ ($\rm cm^{-1}$)	$N_{\rm H,\,opt.}$ ($\rm cm^{-1}$)	A_V	$\beta_{\rm OX}$	$\log(E_{\gamma,\rm iso})$ (erg)	$E_{\rm peak}$ (keV)	Sp. Lag (s)	Ref. z
050126	24.8	1.6	0.00	0.21	0.79	Long	1.29	$(1.1^{+6.5}_{-1.1})\times10^{21}$	–	–	–	$51.70^{+0.15}_{-0.21}$	–	–	1
050223	22.5	1.1	0.00	0.56	0.44	Int.	0.59	–	–	–	–	$50.85^{+0.23}_{-0.07}$	–	–	2
050315	95.5	0.9	0.00	0.08	0.92	Long	1.95	$(8.8^{+2.1}_{-1.0})\times10^{21}$	–	–	0.63	$52.76^{+0.32}_{-0.01}$	–	$0.730^{+0.160}_{-0.220}$	3
050318	32.0	1.0	0.00	0.40	0.60	Long	1.44	$(9.9^{+7.2}_{-3.8})\times10^{20}$	–	0.53 ± 0.00	0.75	52.34 ± 0.03	115 ± 25	–	3
050319	152.4	1.0	0.00	0.02	0.98	Long	3.24	$(9.5^{+23.1}_{-9.5})\times10^{20}$	$(7.9^{+4.6}_{-2.9})\times10^{20}$	0.05 ± 0.09	0.90	$52.66^{+0.38}_{-0.06}$	–	–	4
050401	33.3	1.5	0.00	0.13	0.87	Long	2.90	$(1.4^{+0.7}_{-0.6})\times10^{22}$	$(4.0^{+4.0}_{-2.0})\times10^{22}$	0.69 ± 0.02	0.36	53.55 ± 0.08	467 ± 110	$0.276^{+0.006}_{-0.012}$	4
050416A	2.5	0.5	0.00	1.00	0.00	Int.	0.65	$(5.4^{+0.6}_{-0.8})\times10^{21}$	–	0.21 ± 0.14	0.70	50.98 ± 0.04	28 ± 6	–	5
050505	58.9	1.5	0.00	0.05	0.95	Long	4.27	$(1.6^{+0.4}_{-0.2})\times10^{22}$	–	–		$53.20^{+0.26}_{-0.09}$	–	–	6
050509B	0.1	1.5	1.00	0.00	0.00	Short	0.22	$(1.8^{+1479.1}_{-1.8})\times10^{18}$	–	–	<0.74	48.78 ± 0.20	>183	–	7
050525A	8.8	1.3	0.01	0.85	0.14	Int.	0.61	$(1.5^{+0.8}_{-0.7})\times10^{21}$	–	0.32 ± 0.20	0.92	52.40 ± 0.07	131 ± 4	$0.127^{+0.001}_{-0.009}$	8
050603	12.4	1.8	0.02	0.51	0.47	Int.	2.82	$(4.4^{+2.2}_{-2.9})\times10^{21}$	–	–	–	53.78 ± 0.03	1333 ± 107	$0.058^{+0.001}_{-0.001}$	9
050724	3.0	1.3	0.10	0.89	0.00	Int.	0.26	$(1.3^{+0.6}_{-0.7})\times10^{21}$	–	–	–	50.41 ± 0.12	>126	$0.001^{+0.005}_{-0.001}$	10
050730	156.3	1.4	0.00	0.01	0.99	Long	3.97	–	$(1.3^{+0.3}_{-0.3})\times10^{22}$	0.10 ± 0.01	0.79	$52.95^{+0.28}_{-0.18}$	–	–	4
050801	19.4	1.0	0.00	0.80	0.20	Int.	1.56	–	–	0.30 ± 0.18	0.95	$51.51^{+0.34}_{-0.12}$	–	$0.310^{+0.080}_{-0.080}$	4
050802	19.0	1.4	0.00	0.38	0.62	Long	1.71	$(2.6^{+1.0}_{-1.0})\times10^{20}$	–	0.21 ± 0.13	0.51	$52.26^{+0.28}_{-0.08}$	–	–	4
050813	0.4	1.6	1.00	0.00	0.00	Short	0.72	–	–	–	<1.44	50.89 ± 0.22	>344	–	11
050814	151.0	1.1	0.00	0.01	0.99	Long	5.30	–	–	–	0.51	$52.78^{+0.18}_{-0.08}$	–	–	12
050820A	26.0	1.7	0.00	0.17	0.83	Long	2.61	–	$(1.3^{+0.3}_{-0.3})\times10^{21}$	0.07 ± 0.01	0.77	53.99 ± 0.03	1325 ± 277	–	4
050824	22.6	0.6	0.00	1.00	0.00	Int.	0.83	$(3.7^{+8.2}_{-3.7})\times10^{20}$	–	0.14 ± 0.13	0.91	$51.18^{+0.83}_{-0.13}$	–	–	4
050826	35.5	1.8	0.00	0.14	0.86	Long	0.30	$(8.8^{+1.7}_{-2.3})\times10^{21}$	–	–	–	$50.48^{+0.37}_{-0.48}$	–	–	13
050904	174.2	1.7	0.00	0.01	0.99	Long	6.30	$(3.3^{+7.1}_{-3.3})\times10^{21}$	–	0.02 ± 0.08	<0.41	54.09 ± 0.04	3178 ± 1094	–	14
050908	19.4	1.1	0.00	0.69	0.31	Int.	3.35	–	$(4.0^{+1.0}_{-0.8})\times10^{17}$	–	1.14	$52.11^{+0.23}_{-0.11}$	–	–	4
050922C	4.5	1.5	0.15	0.79	0.06	Int.	2.20	$(2.5^{+1.5}_{-0.8})\times10^{21}$	$(3.5^{+0.9}_{-0.7})\times10^{21}$	0.01 ± 0.01	0.99	52.72 ± 0.12	415 ± 111	$0.141^{+0.006}_{-0.006}$	4
051016B	4.0	0.8	0.00	1.00	0.00	Int.	0.94	$(5.5^{+0.6}_{-1.4})\times10^{21}$	–	–	0.63	$50.57^{+0.40}_{-0.08}$	–	$0.120^{+0.030}_{-0.030}$	15
051109A	37.2	1.4	0.00	0.11	0.89	Long	2.35	$(5.1^{+3.0}_{-2.7})\times10^{21}$	–	0.09 ± 0.03	–	52.81 ± 0.04	539 ± 200	–	16
051109B	14.3	1.0	0.00	0.90	0.10	Int.	0.08	$(1.4^{+0.4}_{-0.7})\times10^{21}$	–	–	–	$48.56^{+0.18}_{-0.12}$	–	–	17
051111	46.1	1.6	0.00	0.07	0.92	Long	1.55	$(6.0^{+1.9}_{-2.3})\times10^{21}$	–	0.18 ± 0.02	–	$52.99^{+0.11}_{-0.08}$	–	$1.460^{+0.100}_{-0.240}$	18
051221A	1.4	1.5	0.87	0.13	0.00	Short	0.55	$(1.6^{+0.4}_{-0.3})\times10^{21}$	–	–	0.70	51.40 ± 0.08	622 ± 35	$0.000^{+0.001}_{-0.001}$	19
060115	139.6	1.1	0.00	0.01	0.99	Long	3.53	–	$(3.2^{+0.8}_{-0.7})\times10^{21}$	–	0.78	52.80 ± 0.06	285 ± 34	–	4
060124	750.0	1.1	0.00	0.00	1.00	Long	2.30	$(6.5^{+1.6}_{-1.5})\times10^{21}$	$(3.2^{+6.8}_{-2.2})\times10^{18}$	0.17 ± 0.03	0.80	53.62 ± 0.06	784 ± 285	–	4
060202	199.1	1.2	0.00	0.01	0.99	Long	0.78	–	–	–	<0.20	$51.85^{+0.27}_{-0.07}$	–	–	20
060206	7.6	1.2	0.01	0.93	0.07	Int.	4.05	$(5.1^{+9.8}_{-5.1})\times10^{21}$	–	0.01 ± 0.02	0.95	52.63 ± 0.09	394 ± 46	$0.560^{+0.040}_{-0.030}$	4
060210	255.3	1.4	0.00	0.00	1.00	Long	3.91	$(1.8^{+0.4}_{-0.2})\times10^{22}$	$(3.5^{+1.5}_{-1.0})\times10^{21}$	1.18 ± 0.10	0.37	$53.79^{+0.06}_{-0.15}$	–	–	4
060218	2100.0	0.8	0.00	0.00	1.00	Long	0.03	$(3.5^{+0.3}_{-0.5})\times10^{21}$	–	–	–	49.73 ± 0.02	4.9 ± 0.3	–	21
060223A	11.3	1.2	0.00	0.82	0.17	Int.	4.41	$(2.7^{+1.5}_{-1.9})\times10^{22}$	–	–	–	$52.00^{+58.00}_{-0.00}$	–	$0.910^{+0.130}_{-0.090}$	22
060319	10.6	0.8	0.00	1.00	0.00	Int.	1.15	–	–	–	<0.41	$51.31^{+0.34}_{-0.09}$	–	–	23

Table 1. continued.

GRB	T_{90} (s)	HR	P1	P2	P3	Type	z	$N_{\rm H,X}$ ($\rm cm^{-1}$)	$N_{\rm H,\,opt.}$ ($\rm cm^{-1}$)	A_V	$\beta_{\rm OX}$	$\log(E_{\gamma,\,\rm iso})$ (erg)	$E_{\rm peak}$ (keV)	Sp. Lag (s)	Ref. z
060418	103.0	1.2	0.00	0.02	0.98	Long	1.49	$(3.5^{+1.7}_{-1.6})\times10^{21}$	–	0.20 ± 0.08	–	53.11 ± 0.08	572 ± 143	$-0.031^{+0.009}_{-0.009}$	24
060502A	28.4	1.4	0.00	0.18	0.82	Long	1.51	$(1.3^{+1.2}_{-1.1})\times10^{21}$	–	0.38 ± 0.14	0.65	$52.57^{+0.20}_{-0.18}$	–	$3.310^{+0.180}_{-0.120}$	4
060502B	0.1	2.1	1.00	0.00	0.00	Short	0.29	–	–	–	<1.04	$49.48^{+0.43}_{-0.48}$	–	–	25
060505	4.0	1.6	0.34	0.60	0.06	Int.	0.09	–	–	~0.00	–	49.41 ± 0.12	>160	–	26
060510B	275.4	1.2	0.00	0.00	1.00	Long	4.90	$(7.9^{+8.8}_{-5.1})\times10^{21}$	–	–	–	$53.36^{+0.16}_{-0.08}$	–	–	27
060512	8.5	0.7	0.00	1.00	0.00	Int.	2.11	–	–	0.56 ± 0.10	0.98	–	–	–	4
060522	71.1	1.4	0.00	0.03	0.97	Long	5.11	$(2.1^{+1.9}_{-1.5})\times10^{22}$	–	–	0.74	–	–	–	28
060526	297.9	1.0	0.00	0.00	1.00	Long	3.21	–	$(1.0^{+0.4}_{-0.3})\times10^{20}$	0.05 ± 0.11	1.03	52.41 ± 0.05	105 ± 21	$0.160^{+0.030}_{-0.030}$	4
060602A	75.0	1.7	0.00	0.04	0.96	Long	0.79	–	–	–	–	$51.98^{+0.16}_{-1.18}$	–	–	29
060605	79.1	1.4	0.00	0.03	0.97	Long	3.77	$(3.4^{+3.9}_{-3.2})\times10^{21}$	–	0.30 ± 0.05	1.00	$52.40^{+0.35}_{-0.12}$	–	–	30
060607A	102.1	1.4	0.00	0.02	0.98	Long	3.08	$(1.6^{+1.4}_{-1.4})\times10^{21}$	$(8.9^{+0.6}_{-0.6})\times10^{16}$	0.08 ± 0.08	0.53	$52.95^{+0.25}_{-0.11}$	–	$0.530^{+0.110}_{-0.110}$	4
060614	5.0	1.4	0.05	0.93	0.01	Int.	0.13	–	–	0.28 ± 0.07	0.79	51.33 ± 0.15	55 ± 45	$0.026^{+0.006}_{-0.006}$	4
060707	66.2	1.2	0.00	0.05	0.95	Long	3.43	–	$(1.0^{+0.6}_{-0.4})\times10^{21}$	–	0.73	52.73 ± 0.08	279 ± 28	–	4
060708	10.2	1.2	0.00	0.83	0.16	Int.	1.92	$(1.9^{+0.9}_{-1.1})\times10^{21}$	–	–	1.04	$51.78^{+0.22}_{-0.08}$	–	–	4
060714	115.1	1.0	0.00	0.02	0.98	Long	2.71	$(9.6^{+3.2}_{-3.0})\times10^{21}$	$(6.3^{+1.6}_{-1.3})\times10^{21}$	–	0.77	$52.89^{+0.30}_{-0.05}$	–	–	4
060729	115.3	1.2	0.00	0.01	0.98	Long	0.54	$(1.2^{+0.2}_{-0.2})\times10^{21}$	–	0.10 ± 0.08	0.80	$51.52^{+0.27}_{-0.09}$	–	–	4
060801	0.5	2.9	1.00	0.00	0.00	Short	1.13	$(6.2^{+4.9}_{-1.9})\times10^{21}$	–	–	–	$51.49^{+0.05}_{-0.05}$	–	–	31
060814	145.2	1.4	0.00	0.01	0.99	Long	0.84	–	–	–	<0.06	52.84 ± 0.04	473 ± 155	$0.330^{+0.020}_{-0.010}$	32
060904B	171.4	1.3	0.00	0.01	0.99	Long	0.70	$(3.6^{+1.1}_{-1.1})\times10^{21}$	–	0.08 ± 0.08	–	$51.71^{+0.13}_{-0.21}$	–	$0.500^{+0.040}_{-0.050}$	4
060906	43.5	1.0	0.00	0.32	0.68	Long	3.68	$(2.5^{+1.4}_{-1.3})\times10^{22}$	$(7.1^{+1.8}_{-1.5})\times10^{21}$	0.05 ± 0.05	–	$53.11^{+0.28}_{-0.03}$	–	–	4
060908	19.3	1.6	0.00	0.30	0.69	Long	1.88	$(6.1^{+3.3}_{-2.6})\times10^{21}$	–	0.05 ± 0.03	0.73	52.99 ± 0.04	514 ± 102	$0.200^{+0.030}_{-0.020}$	4
060912	5.0	1.2	0.02	0.96	0.02	Int.	0.94	$(2.4^{+0.8}_{-0.5})\times10^{21}$	–	–	–	$51.90^{+0.21}_{-0.12}$	–	$0.262^{+0.006}_{-0.006}$	33
060926	8.0	0.7	0.00	1.00	0.00	Int.	3.20	$(3.5^{+2.4}_{-2.0})\times10^{21}$	$(4.0^{+1.6}_{-1.2})\times10^{22}$	–	–	$52.00^{+0.51}_{-0.10}$	–	–	4
060927	22.5	1.2	0.00	0.40	0.60	Long	5.47	$(1.2^{+2.0}_{-1.2})\times10^{22}$	–	0.21 ± 0.09	0.55	53.14 ± 0.06	475 ± 47	$0.062^{+0.015}_{-0.008}$	4
061006	0.5	1.5	1.00	0.00	0.00	Short	0.44	$(1.8^{+1.7}_{-1.8})\times10^{21}$	–	–	–	51.24 ± 0.06	955 ± 259	$0.045^{+0.001}_{-0.006}$	31
061007	75.3	2.0	0.00	0.08	0.92	Long	1.26	$(5.4^{+1.0}_{-0.9})\times10^{21}$	–	0.48 ± 0.10	0.79	53.94 ± 0.04	890 ± 124	$0.237^{+0.006}_{-0.006}$	4
061021	46.2	1.6	0.00	0.08	0.92	Long	0.35	$(7.3^{+1.6}_{-1.0})\times10^{20}$	–	–	0.75	$51.53^{+0.06}_{-0.24}$	–	$0.070^{+0.010}_{-0.010}$	4
061028	106.2	1.2	0.00	0.02	0.98	Long	0.76	$(2.2^{+3.9}_{-2.2})\times10^{21}$	–	–	–	$51.36^{+0.36}_{-0.12}$	–	–	34
061110A	40.7	1.3	0.00	0.12	0.88	Long	0.76	–	–	–	0.99	$51.45^{+0.30}_{-0.10}$	–	–	4
061110B	134.0	2.0	0.00	0.04	0.96	Long	3.44	$(3.0^{+2.5}_{-2.3})\times10^{22}$	–	–	0.55	$53.11^{+0.34}_{-0.27}$	–	–	4
061121	81.3	1.5	0.00	0.03	0.97	Long	1.31	$(4.9^{+0.6}_{-0.5})\times10^{21}$	–	0.42 ± 0.14	0.64	53.35 ± 0.05	1289 ± 153	$0.012^{+0.001}_{-0.001}$	4
061126	70.8	1.6	0.00	0.04	0.96	Long	1.16	$(6.0^{+95.0}_{-0.9})\times10^{21}$	–	0.10 ± 0.06	–	53.48 ± 0.05	1337 ± 410	$0.141^{+0.013}_{-0.006}$	35
061201	0.8	2.3	1.00	0.00	0.00	Short	0.11	–	–	–	0.71	$50.15^{+0.06}_{-0.78}$	–	$0.028^{+0.006}_{-0.009}$	36
061210	0.1	2.3	1.00	0.00	0.00	Short	0.41	–	–	–	–	$51.06^{+0.08}_{-0.41}$	–	$0.003^{+0.001}_{-0.001}$	31
061222A	71.4	1.6	0.00	0.04	0.96	Long	2.09	$(3.2^{+0.3}_{-0.3})\times10^{22}$	–	–	<0.22	$53.50^{+0.08}_{-0.04}$	–	$0.060^{+0.010}_{-0.060}$	31
061222B	40.0	1.0	0.00	0.31	0.69	Long	3.36	$(4.2^{+1.4}_{-2.1})\times10^{22}$	–	–	–	$52.94^{+0.17}_{-0.34}$	–	$5.460^{+0.610}_{-1.310}$	37
070110	88.3	1.3	0.00	0.02	0.98	Long	2.35	$(1.9^{+11.2}_{-1.9})\times10^{20}$	$(5.0^{+1.3}_{-1.0})\times10^{21}$	0.36 ± 0.13	0.77	$52.48^{+0.26}_{-0.08}$	–	–	4
070208	47.8	1.0	0.00	0.20	0.80	Long	1.17	$(5.9^{+1.4}_{-1.9})\times10^{21}$	–	0.74 ± 0.03	0.68	$51.45^{+0.25}_{-0.15}$	–	–	38

Table 1. continued.

GRB	T_{90} (s)	HR	P1	P2	P3	Type	z	$N_{\rm H,X}$ ($\rm cm^{-1}$)	$N_{\rm H,opt.}$ ($\rm cm^{-1}$)	A_V	$\beta_{\rm OX}$	$\log(E_{\gamma,\rm iso})$ (erg)	$E_{\rm peak}$ (keV)	Sp. Lag (s)	Ref. z
070306	209.4	1.3	0.00	0.00	1.00	Long	1.50	–	–	–	<0.23	$52.78^{+0.26}_{-0.08}$	–	$0.440^{+0.040}_{-0.030}$	4
070318	74.6	1.5	0.00	0.03	0.97	Long	0.84	$(5.6^{+0.4}_{-0.5})\times10^{21}$	–	–	0.78	$51.95^{+0.30}_{-0.11}$	–	$0.150^{+0.120}_{-0.090}$	4
070411	121.6	1.2	0.00	0.01	0.99	Long	2.95	$(1.5^{+1.5}_{-1.2})\times10^{22}$	$(2.0^{+2.0}_{-1.0})\times10^{19}$	–	–	$53.00^{+0.26}_{-0.10}$	–	–	4
070419A	115.6	0.8	0.00	0.10	0.90	Long	0.97	$(2.5^{+1.3}_{-0.6})\times10^{21}$	–	0.35 ± 0.29	0.94	$51.38^{+0.29}_{-0.10}$	–	–	4
070429B	0.5	1.2	0.99	0.01	0.00	Short	0.90	–	–	–	<0.92	$50.13^{+0.42}_{-0.20}$	–	$0.032^{+0.013}_{-0.013}$	39
070506	4.3	1.2	0.03	0.96	0.01	Int.	2.31	$(3.0^{+4.8}_{-2.8})\times10^{21}$	$(1.0^{+1.0}_{-0.5})\times10^{22}$	–	0.93	$51.53^{+0.20}_{-0.30}$	–	–	4
070508	20.9	1.6	0.00	0.27	0.73	Long	0.82	–	–	–	–	$52.88^{+0.01}_{-0.03}$	–	$0.060^{+0.001}_{-0.001}$	4
070521	37.9	1.6	0.00	0.10	0.90	Long	1.35	$(1.6^{+0.2}_{-0.2})\times10^{22}$	–	–	<0.06	–	–	$0.173^{+0.013}_{-0.006}$	40
070529	109.1	1.6	0.00	0.02	0.98	Long	2.50	$(1.6^{+0.5}_{-0.6})\times10^{22}$	–	–	–	$52.95^{+0.31}_{-0.18}$	–	–	41
070611	12.2	1.3	0.00	0.73	0.27	Int.	2.04	$(1.5^{+3.8}_{-1.5})\times10^{21}$	–	–	0.73	$51.70^{+0.26}_{-0.10}$	–	–	4
070612A	369.0	1.2	0.00	0.00	1.00	Long	0.62	–	–	–	–	$51.96^{+0.08}_{-0.10}$	–	–	42
070714B	3.0	1.8	0.52	0.48	0.00	Short	0.92	$(4.7^{+1.0}_{-1.2})\times10^{21}$	–	–	–	52.05 ± 0.09	2150 ± 750	$0.013^{+0.001}_{-0.006}$	39
070721B	334.2	1.8	0.00	0.01	0.99	Long	3.63	–	$(3.2^{+1.8}_{-1.2})\times10^{21}$	–	0.72	$53.47^{+0.22}_{-0.18}$	–	–	4
070724A	0.4	1.1	0.99	0.01	0.00	Short	0.46	–	–	0.95 ± 0.05	<0.51	$49.39^{+0.36}_{-0.15}$	–	–	43
070802	16.9	1.2	0.00	0.58	0.42	Int.	2.45	$(1.1^{+0.7}_{-0.9})\times10^{22}$	$(3.2^{+1.8}_{-1.2})\times10^{21}$	1.18 ± 0.19	0.49	$51.70^{+0.31}_{-0.09}$	–	–	4
070809	1.3	1.2	0.61	0.39	0.00	Short	0.22	–	–	1.45 ± 0.30	–	$49.12^{+0.36}_{-0.15}$	–	$-0.010^{+0.010}_{-0.010}$	44
070810A	9.6	0.9	0.00	0.99	0.01	Int.	2.17	$(5.1^{+1.6}_{-2.0})\times10^{21}$	–	–	–	$51.96^{+0.05}_{-0.16}$	–	$0.760^{+0.120}_{-0.080}$	45
071003	148.3	1.6	0.00	0.01	0.99	Long	1.60	–	–	0.40 ± 0.06	–	53.56 ± 0.05	2077 ± 286	$0.070^{+0.010}_{-0.020}$	46
071010A	6.2	0.8	0.00	1.00	0.00	Int.	0.98	–	–	0.64 ± 0.08	–	$51.12^{+0.46}_{-0.08}$	–	–	47
071010B	36.0	1.0	0.00	0.41	0.59	Long	0.95	$(2.4^{+2.2}_{-1.8})\times10^{21}$	–	0.00 ± 0.00	–	52.24 ± 0.18	101 ± 20	$0.160^{+0.010}_{-0.010}$	48
071020	4.2	1.8	0.41	0.54	0.05	Int.	2.15	–	–	0.28 ± 0.08	0.56	52.98 ± 0.16	1013 ± 160	$0.045^{+0.002}_{-0.001}$	4
071025	153.1	1.2	0.00	0.01	0.99	Long	4.80	–	–	–	0.50	$53.81^{+0.19}_{-0.06}$	–	$6.010^{+1.150}_{-1.590}$	4
071031	180.7	0.8	0.00	0.05	0.95	Long	2.69	$(1.4^{+2.6}_{-1.4})\times10^{21}$	$(1.4^{+0.2}_{-0.2})\times10^{22}$	0.14 ± 0.13	0.97	$52.59^{+0.31}_{-0.06}$	–	–	4
071117	6.3	1.4	0.03	0.89	0.08	Int.	1.33	$(1.2^{+0.2}_{-0.3})\times10^{21}$	–	–	0.58	52.61 ± 0.09	647 ± 226	$0.717^{+0.003}_{-0.004}$	4
071122	68.7	1.1	0.00	0.05	0.95	Long	1.14	–	–	0.24 ± 0.23	0.83	$51.54^{+0.39}_{-0.17}$	–	–	49
071227	1.8	2.0	0.91	0.09	0.00	Short	0.38	–	–	–	–	51.01 ± 0.07	1384 ± 277	–	50
080129	53.6	1.5	0.00	0.06	0.94	Long	4.35	$(1.3^{+1.0}_{-1.2})\times10^{21}$	–	0.00 ± 0.00	–	$52.89^{+0.29}_{-0.26}$	–	–	51
080210	43.1	1.2	0.00	0.13	0.87	Long	2.64	$(1.4^{+0.6}_{-0.4})\times10^{22}$	$(7.9^{+2.1}_{-1.6})\times10^{21}$	0.70 ± 0.15	0.74	$52.71^{+0.26}_{-0.08}$	–	–	4
080310	363.9	0.8	0.00	0.01	0.99	Long	2.43	–	$(5.0^{+1.3}_{-1.0})\times10^{18}$	0.19 ± 0.05	0.88	$52.77^{+0.45}_{-0.08}$	–	–	4
080319B	122.7	1.9	0.00	0.04	0.96	Long	0.94	$(1.1^{+0.3}_{-0.3})\times10^{21}$	–	0.07 ± 0.06	0.67	54.06 ± 0.03	1261 ± 65	$0.037^{+0.001}_{-0.001}$	4
080319C	29.7	1.6	0.00	0.16	0.84	Long	1.95	$(7.6^{+2.0}_{-1.9})\times10^{21}$	–	0.59 ± 0.12	0.31	53.15 ± 0.08	906 ± 272	$0.190^{+0.010}_{-0.010}$	4
080330	67.0	0.9	0.00	0.21	0.79	Long	1.51	–	–	0.16 ± 0.11	0.99	$51.62^{+0.51}_{-0.07}$	–	–	4
080411	56.4	1.3	0.00	0.06	0.94	Long	1.03	$(4.4^{+0.4}_{-0.3})\times10^{21}$	–	–	–	53.19 ± 0.03	524 ± 70	$0.248^{+0.002}_{-0.001}$	4
080413A	46.3	1.4	0.00	0.08	0.92	Long	2.43	$(3.8^{+4.8}_{-3.8})\times10^{21}$	$(7.1^{+2.9}_{-2.1})\times10^{21}$	0.13 ± 0.17	–	52.91 ± 0.10	584 ± 180	$0.160^{+0.010}_{-0.010}$	4
080430	14.3	1.2	0.00	0.71	0.28	Int.	0.76	$(3.4^{+0.4}_{-0.4})\times10^{21}$	–	0.17 ± 0.10	0.77	$51.58^{+0.25}_{-0.10}$	–	$0.440^{+0.020}_{-0.020}$	52
080520	2.8	0.5	0.00	1.00	0.00	Int.	1.55	$(1.4^{+0.4}_{-0.6})\times10^{22}$	–	–	0.77	$51.04^{+1.15}_{-0.20}$	–	–	4

Table 1. continued.

GRB	T_{90} (s)	HR	P1	P2	P3	Type	z	$N_{\rm H,X}$ ($\rm cm^{-1}$)	$N_{\rm H,\,opt.}$ ($\rm cm^{-1}$)	A_V	$\beta_{\rm OX}$	$\log(E_{\gamma,\,\rm iso})$ (erg)	$E_{\rm peak}$ (keV)	Sp. Lag (s)	Ref. z
080603B	59.0	1.2	0.00	0.07	0.93	Long	2.69	$(8.5^{+6.7}_{-5.7}) \times 10^{21}$	$(7.1^{+0.9}_{-0.8}) \times 10^{21}$	–	0.92	53.04 ± 0.01	376 ± 100	$0.120^{+0.010}_{-0.010}$	4
080604	82.0	1.2	0.00	0.03	0.97	Long	1.42	$(5.9^{+13.2}_{-5.9}) \times 10^{20}$	–	–	0.90	$51.85^{+0.33}_{-0.07}$	–	–	4
080605	19.1	1.6	0.00	0.31	0.69	Long	1.64	$(6.6^{+2.0}_{-1.8}) \times 10^{21}$	–	–	0.38	53.38 ± 0.03	650 ± 55	$0.102^{+0.001}_{-0.006}$	4
080607	79.8	1.8	0.00	0.05	0.95	Long	3.04	$(2.6^{+0.4}_{-0.4}) \times 10^{22}$	$(5.0^{+2.1}_{-1.5}) \times 10^{22}$	3.20 ± 0.50	0.24	54.27 ± 0.02	1691 ± 226	$0.160^{+0.006}_{-0.001}$	4
080707	30.2	1.2	0.00	0.28	0.72	Long	1.23	$(3.3^{+1.8}_{-1.8}) \times 10^{21}$	–	–	0.83	$51.53^{+0.34}_{-0.07}$	–	–	4
080710	113.8	1.5	0.00	0.01	0.98	Long	0.85	$(1.2^{+0.5}_{-0.3}) \times 10^{21}$	–	0.11 ± 0.04	1.04	$51.90^{+0.31}_{-0.32}$	–	–	4
080804	33.6	1.8	0.00	0.16	0.84	Long	2.20	$(2.3^{+1.3}_{-1.2}) \times 10^{21}$	$(2.0^{+0.8}_{-0.6}) \times 10^{21}$	–	0.78	$53.20^{+0.31}_{-0.25}$	–	–	4
080805	105.7	1.4	0.00	0.01	0.98	Long	1.51	$(1.1^{+0.3}_{-0.4}) \times 10^{22}$	–	–	0.40	$52.60^{+0.18}_{-0.30}$	–	$8.600^{+0.450}_{-0.620}$	4
080810	108.6	1.7	0.00	0.02	0.98	Long	3.35	$(3.7^{+2.7}_{-2.6}) \times 10^{21}$	–	0.16 ± 0.05	0.96	53.65 ± 0.05	1470 ± 180	$-0.160^{+0.060}_{-0.060}$	4
080905A	1.0	2.3	1.00	0.00	0.00	Short	0.12	$(1.6^{+1.0}_{-1.0}) \times 10^{21}$	–	–	–	–	–	$0.004^{+0.017}_{-0.017}$	53
080905B	94.8	1.3	0.00	0.02	0.98	Long	2.37	–	–	–	0.64	$51.85^{+0.41}_{-0.37}$	–	$-0.250^{+0.040}_{-0.030}$	4
080913	7.5	1.6	0.05	0.74	0.21	Int.	6.70	$(3.4^{+5.3}_{-3.4}) \times 10^{22}$	–	~ 0.00	<0.48	52.93 ± 0.11	710 ± 350	–	4
080916A	56.6	1.3	0.00	0.05	0.95	Long	0.69	$(6.3^{+1.2}_{-1.0}) \times 10^{21}$	–	–	0.69	52.01 ± 0.03	184 ± 18	$1.030^{+0.060}_{-0.060}$	4
080928	281.2	1.2	0.00	0.00	1.00	Long	1.69	$(3.0^{+0.0}_{-0.0}) \times 10^{21}$	–	0.14 ± 0.08	1.00	$52.45^{+0.27}_{-0.09}$	–	$0.010^{+0.030}_{-0.040}$	4
081007	8.0	0.7	0.00	1.00	0.00	Int.	0.53	$(5.2^{+0.7}_{-0.6}) \times 10^{21}$	–	–	–	51.19 ± 0.09	61 ± 15	–	54
081008	185.8	1.3	0.00	0.01	0.99	Long	1.97	$(5.7^{+15.1}_{-5.7}) \times 10^{20}$	–	–	–	52.98 ± 0.04	261 ± 52	$0.030^{+0.080}_{-0.080}$	55
081028	281.8	1.1	0.00	0.00	1.00	Long	3.04	–	–	–	–	53.24 ± 0.04	234 ± 93	–	56
081029	275.4	1.5	0.00	0.00	1.00	Long	3.85	$(4.8^{+3.3}_{-3.8}) \times 10^{21}$	–	–	–	$53.18^{+0.20}_{-0.27}$	–	–	57
081118A	47.3	0.9	0.00	0.40	0.60	Long	2.58	–	–	–	–	52.63 ± 0.08	147 ± 14	–	58
081121	16.9	1.8	0.01	0.37	0.62	Long	2.51	–	–	–	–	53.41 ± 0.08	871 ± 123	–	59
081203A	112.2	1.4	0.00	0.01	0.99	Long	2.05	$(5.4^{+1.7}_{-1.5}) \times 10^{21}$	–	0.09 ± 0.04	–	$53.54^{+0.18}_{-0.15}$	–	$1.070^{+0.200}_{-0.280}$	60

Notes. P1, P2, and P3 are the probabilities of belonging to the short, intermediate and long groups respectively. The last column gives the references for the redshifts as follows, while the rest of references are given within the text.

References. (1) Berger et al. (2005a); (2) Pellizza et al. (2006); (3) Berger et al. (2005b); (4) Fynbo et al. (2009); (5) Soderberg et al. (2007); (6) Berger et al. (2006b); (7) Bloom et al. (2006); (8) Della Valle et al. (2006b); (9) Berger & Becker (2005); (10) Berger et al. (2005c); (11) Prochaska et al. (2006a); (12) Jakobsson et al. (2006b); (13) Mirabal et al. (2007); (14) Kawai et al. (2006); (15) Soderberg et al. (2005); (16) Quimby et al. (2005); (17) Perley et al. (2006); (18) Penprase et al. (2006); (19) Soderberg et al. (2006); (20) Butler (2007); (21) Pian et al. (2006); (22) Berger et al. (2006a); (23) Perley & Kemper (2008); (24) Prochaska et al. (2006b); (25) Bloom et al. (2007); (26) Thöne et al. (2008); (27) Price et al. (2007); (28) Cenko et al. (2006); (29) Jakobsson et al. (2007); (30) Ferrero et al. (2009); (31) Berger et al. (2007b); (32) Thöne et al. (2007a); (33) Jakobsson et al. (2006a); (34) Kocevski & Butler (2008); (35) Perley et al. (2008a); (36) Stratta et al. (2007); (37) Berger (2006); (38) Cucchiara et al. (2007b); (39) Cenko et al. (2008); (40) Perley et al. (2009); (41) Berger et al. (2007a); (42) Cenko et al. (2007b); (43) Kocevski et al. (2010); (44) Perley et al. (2008b); (45) Thöne et al. (2007b); (46) Perley et al. (2008c); (47) Prochaska et al. (2007); (48) Cenko et al. (2007a); (49) Cucchiara et al. (2007a); (50) D'Avanzo et al. (2009); (51) Greiner et al. (2009); (52) de Ugarte Postigo et al. (2008); (53) Rowlinson et al. (2010); (54) Berger et al. (2008b); (55) D'Avanzo et al. (2008); (56) Berger et al. (2008a); (57) D'Elia et al. (2008a); (58) D'Elia et al. (2008b); (59) Berger & Rauch (2008); (60) Kuin et al. (2009).